energies

MDPI

Article

Centralized Microgrid Control System in Compliance with IEEE 2030.7 Standard Based on an Advanced Field Unit

Soheil Pouraltafi-kheljan [1], Mesut Ugur [2], Efecan Bozulu [2], Bahadir Can Çalişkan [3], Ozan Keysan [1] and Murat Gol [1,*]

[1] Electric-Electronic Engineering Department, Middle East Technical University, Çankaya, Ankara 06800, Turkey; soheil.kheljan@metu.edu.tr (S.P.-k.); keysan@metu.edu.tr (O.K.)
[2] Earsis Technologies Ltd., METU Technopolis, Çankaya, Ankara 06800, Turkey; mugur@earsis.com (M.U.); ebozulu@earsis.com (E.B.)
[3] Research and Development Department, Başkent EDAŞ Electricity Distribution Inc., Ankara 06460, Turkey; Bahadircan.CALISKAN@baskentedas.com.tr
* Correspondence: mgol@metu.edu.tr; Tel.: +90-312-210-4539

Abstract: The necessity for the utilization of microgrids emerges from the integration of distributed energy resources, electric vehicles, and battery storage systems into the conventional grid structure. In order to achieve a proper operation of the microgrid, the presence of a microgrid control system is crucial. The IEEE 2030.7 standard defines the microgrid control system as a key element of the microgrid that regulates every aspect of it at the point-of-interconnection with the distribution system, and autonomously manages operations such as the transitions of operating modes. In this paper, a microgrid control system is developed to achieve real-time monitoring and control through a centralized approach. The controller consists of a centralized server and advanced field units that are also developed during this work. The control functions of the centralized server ensure the proper operation during grid-connected and island modes, using the real-time data received via the advanced field unit. The developed server and the field unit constitute a complete system solution. The server is composed of control function and communication, database, and user interface modules. The microgrid control functions comprise dispatch and transition core-level functions. A rule-based core-level dispatch function guarantees the security of supply to critical loads during the islanded mode. The core-level transition function accomplishes a successful transition between the operation modes. Moreover, a communication framework and a graphical user interface are implemented. The presented system is tested through thecases based on the IEEE 2030.8 standard.

Keywords: microgrid; central microgrid controller; rule-based dispatch; state of charge (SOC) management; synchrophasor measurements; smart grids

Citation: Pouraltafi-kheljan, S.; Ugur, M.; Bozulu, E.; Çalişkan, B.C.; Keysan, O.; Gol, M. Centralized Microgrid Control System in Compliance with IEEE 2030.7 Standard Based on an Advanced Field Unit. *Energies* **2021**, *14*, 7381. https://doi.org/10.3390/en14217381

Academic Editors: Nikolaos M. Manousakis and Adel Merabet

Received: 13 September 2021
Accepted: 1 November 2021
Published: 5 November 2021

1. Introduction

Microgrids (MG) can be defined as distributed power systems that operate either in grid-connected or island mode [1]. An MG's most commonly recognized factors are the control framework for generation and demand, well-defined limits, and islanding capabilities [1,2]. MGs are primarily electrical, including AC, DC, or hybrid systems, but they can also include thermal components for heating. Because the difference of load generation points is small, the system's norms are less than the main network. MGs enable the combined operation of distributed energy resources (DERs) and energy storage systems considering system reliability [3]. MGs enable the combined operation of distributed energy resources (DERs) and energy storage systems considering system reliability. Integration of MG is expected to solve most of the technical problems caused by the integration of DERs. As a result, the necessity for central coordination will reduce, and the realization of the smart grid will be more straightforward.

Control and operation in an MG are critical factors in the success of electrical systems due to numerous restrictions, such as control functionality in islanded operation or power exchange with the main grid. This system layer may be composed of only the software or both software and hardware. In MG control, a hierarchical control including primary, secondary, and tertiary levels should be followed.

Primary control is the fastest control mechanism, thanks to its local measurements and communication-free approach. Therefore, control of unit connection status, output voltage control, and output power balance control is achieved with this control method [4,5]. While the main grid controls the voltage magnitude and frequency, the main control parameters are the active and reactive power output of the DERs in grid-connected mode. However, in island mode, there is no reference voltage for DERs, so this mode is quite challenging. Even a short duration of voltage and frequency inconsistency may result in large current circulation [6,7].

Secondary control is a more sophisticated control step. Second level control is responsible for supervising and monitoring the system and adjusting for voltage and frequency abnormalities. Indeed, the secondary control guarantees that the frequency and voltage variations in the MG are controlled towards zero after each load or generation fluctuation [8]. This level of control hierarchy can also be denoted as the energy management system (EMS) [9]. This control level can have centralized, decentralized, or distributed architectures. [10].

Most of the existing MG control test benches focus on one specific function, and the tests are conducted without regard to a recognized standard. The MG energy management system coordinates the active and reactive power dispatch setpoints for the inter-dispatch intervals with the local primary power control loops used by the DERs [3]. In [11], an MG control system (MGCS) is validated with a dispatch function on a real-time testbed, but offline optimization is still performed. Similarly, Manson et al. [12] present dispatch and protection functions, but no complete tests are undertaken. For grid-connected and islanded operation modes, Manson et al. propose [12] a control technique that uses an energy storage system (ESS) for power smoothing, keeping the state of charge (SOC) around 50%. Although the SOC can be tightly regulated, it is relatively conservative because the capabilities of ESS as an energy buffer for peak shaving and valley filling are not fully explored. In [13], a comparison of load-following control and cycle-charging control is performed on an islanded PV-diesel-ESS MG, where the ESS and diesel generator are used as the primary sources to achieve power balance. It has been discovered that using ESS to track load change might minimize fuel usage, although the energy stored in the system may be depleted sooner than expected [14]. The lifespan of ESS will be shortened by using a traditional cycle-charging approach with repeated deep discharges. Bo Zhao et al. [15] describe a hybrid adaptive rule-based dispatch for a realistic stand-alone MG that used a diesel generator and energy storage to address power shortfall in several SOC ranges. The control approach, on the other hand, is still unable to achieve its objectives.

Standards contribute to the advancement of MG installation and configuration by having a comprehensive technical basis for interconnection and interaction with the utility grid at the point of interconnection. There are six main standards related to MGs [16]. The IEC 62898 series includes IEC 62898-1 [17] and IEC 62898-2 [18]. IEC 62898-1 covers the technical requirements and guidelines for the MG planning stage. IEC 62898-1 is intended to provide the principles and requirements related to components, operation, and transitions. The IEEE 1547.4 standard [19] provides a reference for the design, operation, and transition of DER, such as the transition to island mode, island mode operation, or the reconnection mode, which can be referred to as an MG. A new version of this standard, IEEE 1547-2018 [20], was published in 2018. The IEEE 2030.7 standard [21] defines and specifies the MGCS as a critical element of the MG that regulates every aspect of the MG at the POI with the distribution system. This system consists of control functions that present the MG as a single entity that can operate autonomously in an island or grid-connected mode. The detailed description of this document is presented in the following

subsection. The IEEE 2030.7 standard cites the IEEE 2030.8 [22] standard to qualify, verify and evaluate the recommended specifications and functionalities. As a result of these tests, MG controllers may be adopted more broadly.

Razeghi et al. [23] proposed the idea of a generic MG controller-based IEEE 2030.7 standard in their report for the U.S. Department of Energy; however, no details of the dispatch function are disclosed. A model-driven generic controller is presented in [24]. This controller is independent of the model of a specific MG system. A digital twin is the byproduct of a model-driven product that may be utilized as a genuine model of an MG controller within simulations. Nonetheless, the details of the utilized model and optimization in their study are missing, and the core-level functions do not include transition functions.

Sun et al. [25] developed a core-level rule-based dispatch function that is in compliance with the IEEE 2030.7 standard. Their proposed controller consists of a weighted and queuing (W&Q) algorithm to apportion the required load shedding or renewable curtailment among the corresponding assets. This algorithm utilizes forecasts of load and generation. However, the IEEE 2030.7 standard does not allow the use of forecasts as part of core-level functions. Additionally, the diesel generator is kept ON unless it is in the force-discharging mode. However, the diesel generator can be utilized to decrease the amount of probable load shedding. In their other work, Sun et al. [26] have proposed a centralized MG control system with rule-based dispatch and seamless transition functions. The control strategy has been implemented with control hardware in the loop (C-HIL) test bench. The method keeps the BSS SOC around 50% for the sake of MG resiliency and reliability and to extend the BSS lifetime. Moreover, a dispatchable DG is kept ON during the operating modes of the MG Load management strategy, but it is not clearly described whether loads are restored after shedding.

The ubiquitous nature of real-time monitoring and control across the nodes of the system differentiates a smart MG from a conventional system. This requires relevant MG nodes to have the capability of generating real-time data and the capability of communicating with other nodes across the system, regardless of where these nodes are or what their functions may be. In other words, monitoring and control within a smart MG system must be an end-to-end exercise encompassing (preferably) all network nodes. That requirement calls for command and control strategies capable of dealing with MG events through localized intelligence. Besides, individual components, such as energy converters, batteries, etc., may have their dedicated management and control intelligence interfacing with the higher-level control systems and applications to receive setpoints and inform them of their status and events [27].

In our approach, the real-time monitoring and control action will be performed through the developed advanced field unit, namely the MG control and communication device (MCCD) and controller multi-thread server (CMTS). The CMTS processes the received data through the novel control functions. These control functions are dispatch and transition core-level functions. The generic dispatch function is established based on SOC-following dispatch rules and load management strategy. The load management strategy sheds and restores the determined amount of load regarding the criticality and controllability of loads. It should be noted that there are load management approaches in other studies; however, those are not in compliance with the specifications of IEEE standards for core-level functions. These control functions make the proposed MGCS flexible for different MGs regardless of an MG's size and application.

In the proposed MGCS, CMTS communicates with MCCDs located in the field through the TCP/IP sockets. Additionally, a graphical user interface (GUI) is provided to the users in the control center.

The main objectives and contributions of this study are as follows:

1. The MG control and communication device is designed and implemented. This device measures the required electrical quantities and applies executed digital and analog commands to the MG assets;

2. Reliable operation for the prioritized (critical) loads rather than the economic operation is of the MG is realized during island mode steady-state by the MG central control system;
3. Loads are classified regarding criticality and controllability, and load management strategy has been developed based on this classification;
4. The proposed method performs successful transition modes, including unplanned islanding (T1) and planned islanding (T2);
5. A proper communication framework between the CMTS and MCCD is implemented;
6. The proposed system provides a graphical user interface for data visualization and manual control for MG operators.

The design details of all corresponding components will be given in the second section and Appendix A. The presented central MG control system is examined through the test cases based on the IEEE 2030.8 standard [22] and the results in the third section.

IEEE 2030.7 Standard

This standard addresses the functions higher than the component control level related to the proper operation of the MG energy management system common to all MGs, regardless of the application, topology, configuration, or administration. This standard levels the control functions into the high, core, and low levels. The scope of this standard is to address the functions above the component control level associated with the proper operation of the MG energy management system that is common to all MGs, regardless of topology, configuration, or jurisdiction. There is a single limitation on MG topology: the MG shall connect to the distribution grid at the POI. The standard declared three distinct characteristics for any system to be considered as an MG:

1. Clearly defined electrical boundaries;
2. A control system to manage and dispatch resources as a single controllable entity;
3. The installed generation capacity exceeds the critical load.

The MGCS includes the control functions that define the MG as a system that can manage itself, operate autonomously or grid-connected, and seamlessly connect to and disconnect from the main distribution grid to exchange power. It satisfies the interconnection requirements using functions at the high level, core level, or low level of its function, and the corresponding stack is given in Figure 1. The lower level, or device-related control action, is performed via the network components' local control.

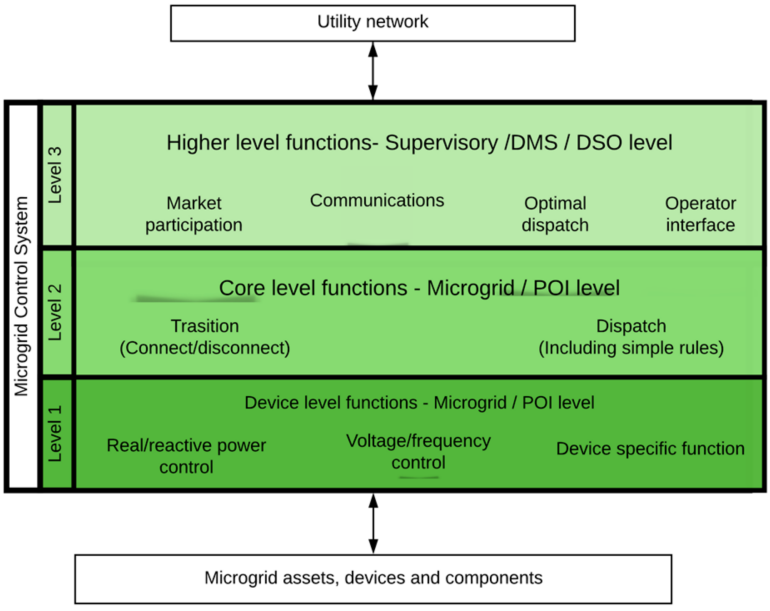

Figure 1. Microgrid control system functional framework.

The main goal of building the core functions is to provide a framework in order to have a modular design of the MG control system employing the platform-independent interfaces. This standard defines functions and their interrelationships that allow modularity and interoperability in physical implementations. It deals with the operation of the MG control system and defines those aspects that need to be standardized; others can remain proprietary. The core-level functions include:

1. The dispatch function: dispatches individual devices in given operating modes and with specified setpoints;
2. The transition function: supervises the transitions between connected and disconnected states and ensures the dispatch is appropriate for the given state.

The dispatch function computes its dispatch order based on a dispatch rule. In the simplest case, this rule is static and set up by the operator at the beginning. A value-added dispatch optimizer engine would be considered a higher-level function and optimizes dispatch by editing the dispatch rule in real-time. This modularizes the optimizer and dispatch functions, making modifications and upgrades of the optimizer easier.

2. The Microgrid Structure

The considered MG assets in this approach are a battery storage system (BSS), a diesel generator (DG), a photovoltaic (PV) system, a set of different loads, and a circuit breaker (CB) at the POI. The corresponding connections and power flow direction are illustrated in Figure 2.

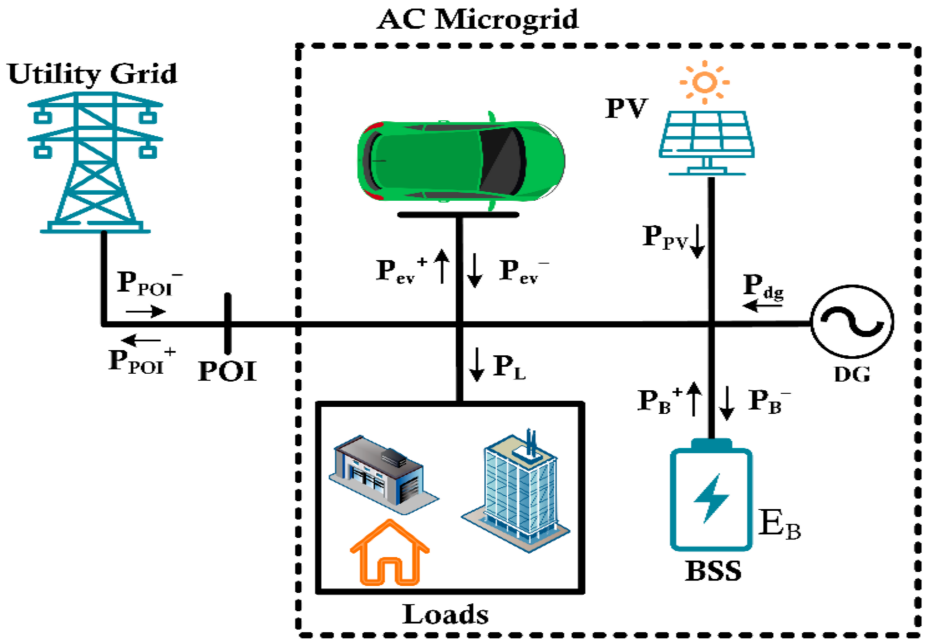

Figure 2. The scheme of the considered MG: illustration of MG boundaries and positive power directions.

The DG has a local frequency-droop (frequency-power) response [20] that is not dispatchable, which is the most common control scheme for DG. However, DG can turn ON/OFF via the MCCD. The BSS employs *Vf* control during the islanded operation mode [26,28], providing voltage and frequency reference for other assets' local controllers. The parameters related to the DG and BSS are given in Table 1. K_d and K_c are adjustable variables to determine minimum discharging and charging power, respectively. In compliance with the IEEE standard's specifications, the proposed control system is developed as a generic one, which means that the proposed method can operate without any component, except for the BSS, and it is not a case-specific control system.

Table 1. The parameters related to DG and BSS.

Asset	Parameter	Description
Diesel generator	t_{min}	Minimum DG ON time (s)
	t_{dg}	DG ON time (s)
	S_{dg}	DG status ON:1, OFF: 0
	P_{dg}^{min}	Minimum generation power (W)
	P_{dg}^{max}	Maximum generation power (W)
Battey storage system	SOC_{min}	The lower limit for SOC(%)
	SOC_{max}	The upper limit for SOC(%)
	P_{ch}^{max}	Maximum charging power (W) $P_{ch}^{max} > 0$
	P_{dis}^{max}	Maximum discharging power (W) $P_{dis}^{max} < 0$
	K_c	Minimum [1] charging power (W)
	P_{dis}^{max}	Minimum [1] discharging power (W)

[1] $K_c, K_d \in [0, 1]$.

The load of MG can be classified from two perspectives: criticality and controllability. In terms of criticality [21], loads can be categorized as follows:

1. Critical loads: These loads should be supplied in all normal operation modes of MG and cannot be shed (P_{ld}^{crt});
2. Priority loads: These sets of loads can be shed or interrupted, but it is not preferred;
3. Interruptible loads: These sets of loads can be shed or interrupted at any time.

Furthermore, regarding controllability, loads can also be divided into two groups: discretely controlled loads (DCL) and continuously controlled loads (CCL).

3. The Microgrid Control System

The interaction between the two main components of the proposed MGCS and corresponding data flow is illustrated in Figure 3. The main data flow is among the MCCD and the CMTS. The MCCD provides frequency, phasor, power measurements, circuit breaker (CB) status, MCCD status, and controlled devices' status. MCCDs are not the single information source for the MGCS. The distribution system operator (DSO) can also send information to the MGCS.

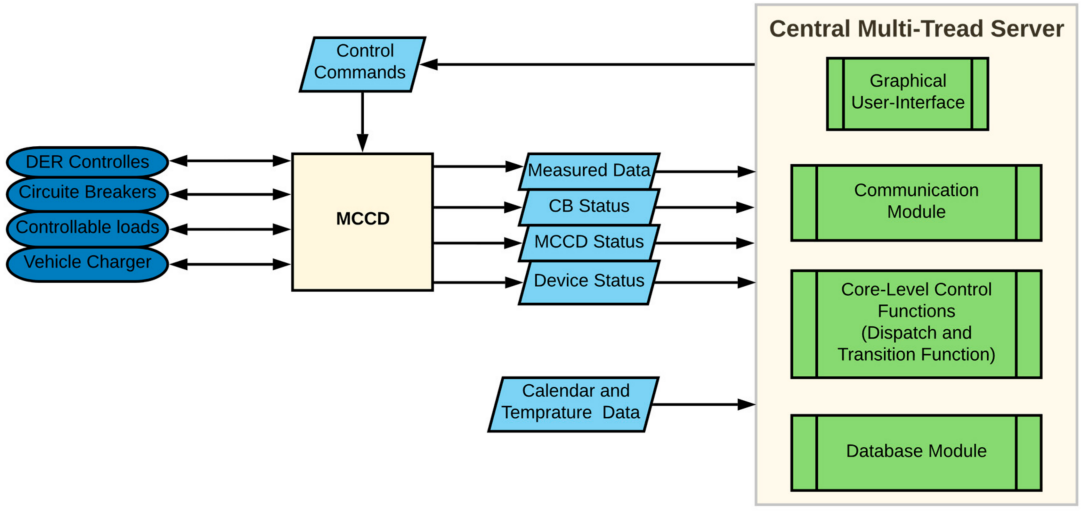

Figure 3. Data flow and interaction within main parts of the MGCS.

Commands executed through the control functions or user interface are transmitted from the CMTS to the MCCD by a communication module. In addition, information such

as formal calendar, academic calendar, and weather conditions are also provided to the CMTS. The description of the MCCD and core-level functions will be illustrated in the following subsections. Details on the database, communication modules, and user interface are given in Appendix A.

The MGCS includes the control functions that define the MG as a system that can autonomously manage itself, either in islanded or in grid-connected mode. It satisfies the interconnection requirements using functions at the high, core, or low level of its function stack. The lower-level functions representing DER/load/devices level functions are not considered in the proposed MGCS because related control actions are performed via network components' local control.

Control system core level functions designate the MG as an independent autonomously controllable system satisfying the DSO and MG operator's (MGO) requirements. The main aim of establishing this function is to have a functionality-driven controller emphasizing the modularity of MGCS. This feature is achieved via platform-independent interfaces. MGCS's functional framework, determined by the IEEE 2030.7 standard, is shown in Figure 1. The functions designated as core functions in this standard pave the way for a modular design of MG control systems.

Two core functions are specified in this standard: the dispatch function and the transition function. The dispatch function operates on a longer time frame than the transition function of the MG, typically in minutes, compared to milliseconds for the transition function. The relationship and interaction between the dispatch and transition functions and control levels are illustrated in Figure 4.

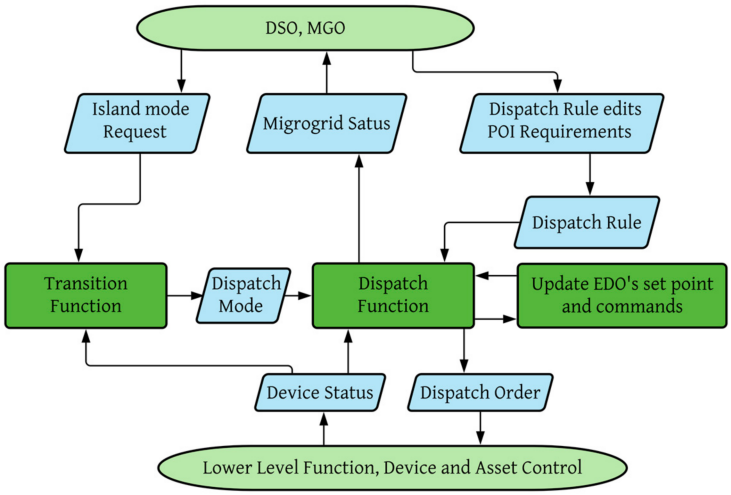

Figure 4. Relationship between transition and dispatch functions.

In the present approach, the dispatch rule is a set of rules for four dispatch modes, which are:

1. Steady-state grid-connected mode (SS1);
2. Steady-state islanded mode (SS2);
3. Unplanned islanding (T1);
4. Planned islanding (T2).

3.1. The Developed Microgrid Control and Communication Device

A field unit is necessary to collect the essential measurements from the MG assets and transmit the required commands from the CMTS. The received commands by the field unit include the control commands that are applied by the MCCD or the MG components, including the CB control command and DER setpoints for dispatchable assets.

Based on those requirements, the MCCD is designed, and a prototype is fabricated. The components and modules of MCCD are illustrated in Figure 5. This device can be

energized using a 1-phase AC socket or a 24 V DC supply. The power consumption of the device is 12 W max. MCCD consists of a synchro-phasor measurement unit to measure and collect data from different MG nodes and components. This device has three measurement channel groups, and each one is intended to be used for a three-phase system. Each group can measure frequency, three fundamental line-to-neutral voltage, and four fundamental current phasors. In total, the device can measure nine voltages and twelve currents with a sampling rate of 15,625 Hz. The measurement range of this device is given in Table 2. It should be noted that the measurement range of current magnitude depends on the ratio of the utilized current transformer.

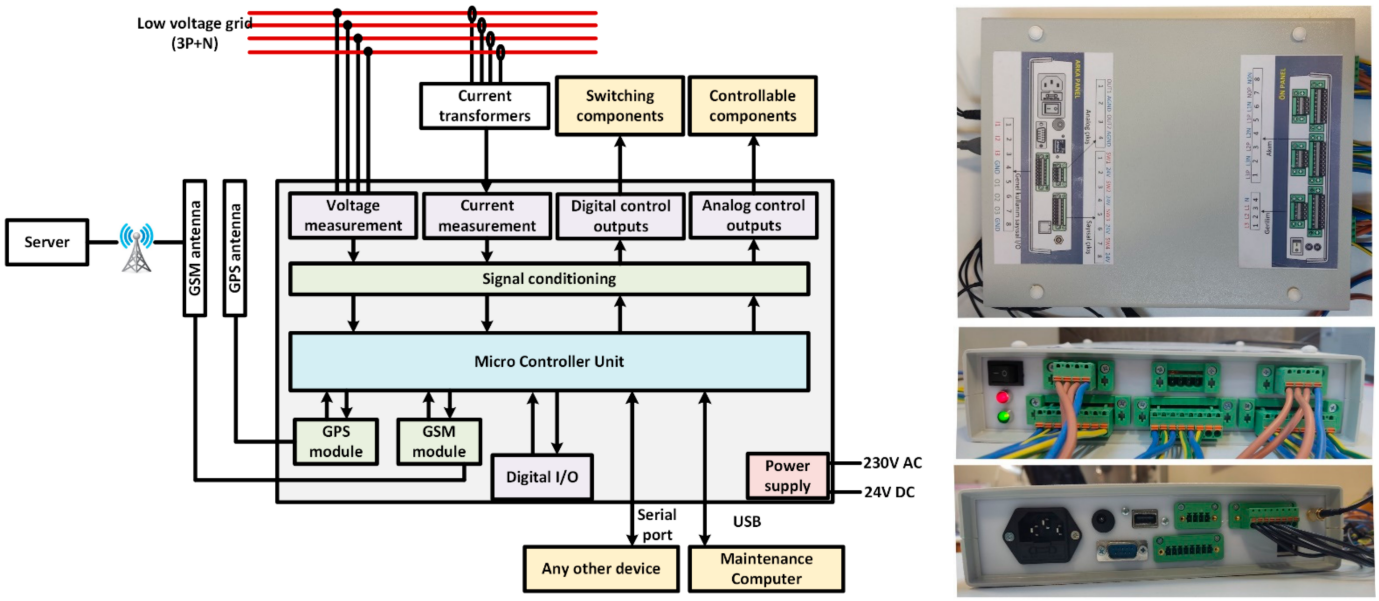

Figure 5. The developed microgrid control and communication device: (**a**) Block scheme of the MCCD. (**b**) fabricated prototype of MCCD.

Table 2. Measurement range of MCCD for voltage and current magnitudes.

Measured Value	Maximum
Voltage magnitude	300 (V)
Current magnitude	1 or 5 (A)

The GPS module enables the device to determine its global location and a time reference for phase angle calculation. Phasor angle calculations are based on the frequency, and the real GPS clock received via the GPS module. The reference system of each device will be the same in terms of phase angle in case of the installation of multiple MCCDs. The block scheme for the measured values calculation algorithm is presented in Figure 6. Frequency is calculated using one of the phase voltages using the second-order generalized–frequency locked loop (SOGI-FLL) algorithm. The calculated frequency is used later to determine the reference angle for the calculation of phasors. The direct and quadrature (D and Q) components of each voltage and current that are referenced to the primary frequency are calculated in the single-phase DQ transform block. All voltage and current quantities are considered independent from each other. Therefore, in-phase and orthogonal signals are calculated for each quantity using SOGI-FLL. Using these orthogonal signals, the D and Q components are found using the Park transformation. The reference angle used in this transformation is obtained using a real-time clock (from GPS) and the aforementioned reference frequency.

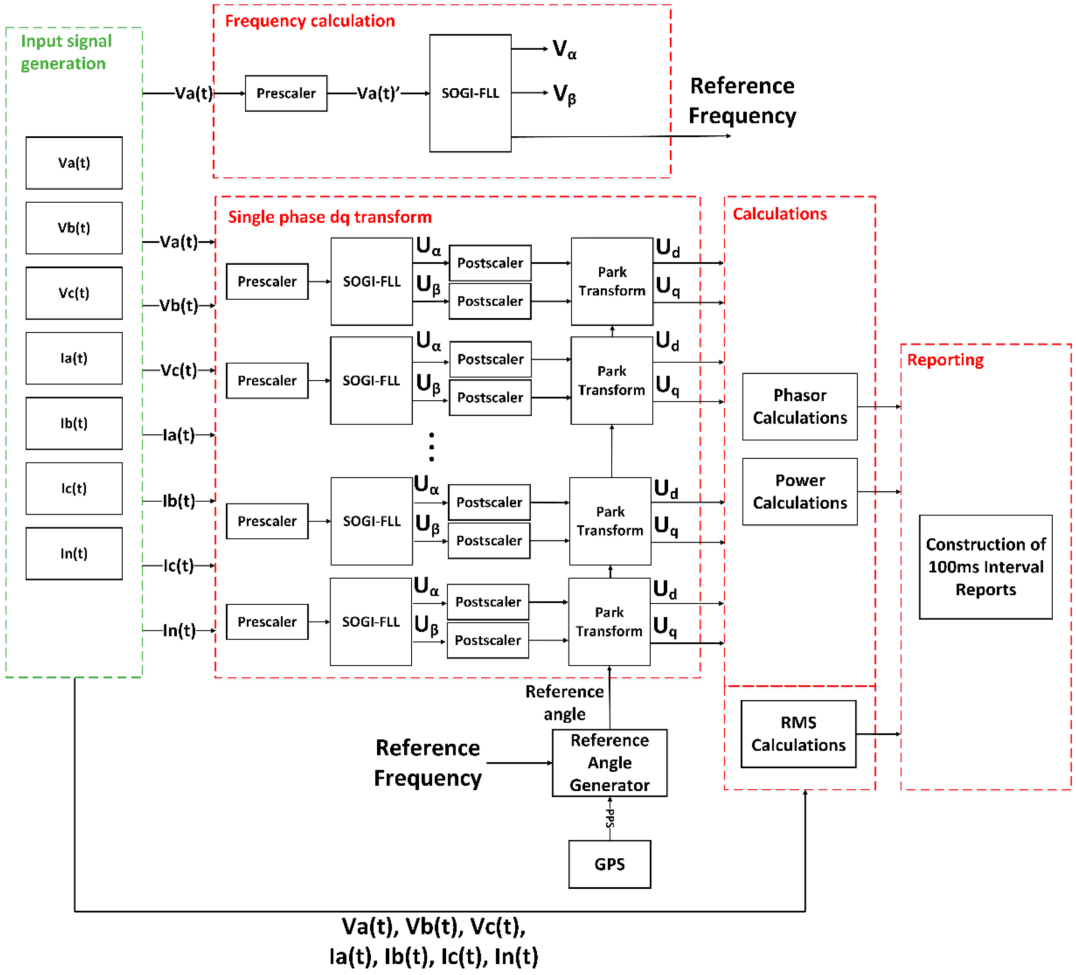

Figure 6. Block scheme of the phasor, frequency, power, and RMS calculation algorithm.

3.2. The Dispatch Function

The dispatch function computes and executes the dispatch orders, which are setpoints of DERs and controllable loads, and CB status based on a dispatch rule. This function acquires the MG operating mode and assets information from the transition function and MCCD, respectively. In summary, the desired functionality of dispatch core function can be expressed as follows [21]:

1. During SS2, load and generation are balanced;
2. During SS1 and SS2, controllable assets are re-dispatched in reaction to the inside events related to the load and generation status;
3. During SS1 and SS2, external commands and events, including MG operator and DSO, are handled, and if necessary, controllable assets are re-dispatched.

Chu Sun et al. [26] developed a hybrid rule-based dispatch strategy as an MG central controller. The method keeps the BSS SOC around 50% for the sake of MG resiliency and reliability and to extend the BSS lifetime. Moreover, a dispatchable DG is kept ON during the operating modes of the MG. Three control modes for the dispatch strategy are allocated based on overlapped SOC ranges. In the proposed approach, a similar control allocation is adopted; however, the DG is not dispatchable, and it is off during SS1, and if necessary, it can be switched ON or OFF to decrease load shedding or renewable curtailment during SS2. Three SOC overlapped ranges are illustrated in Figure 7a. Four adjustable parameters (SOC_{dl} , SOC_{d} , SOC_{u}, and SOC_{ul}) are used to define SOC ranges. Each SOC range corresponds to a control rule, which are force-charging, power-smoothing, and force-discharging. This control allocation logic is applied for dispatch function in SS2

(Conditions A, B, and C) and SS1 (A' , B', and C'). In the algorithm shown in Figure 7b, another parameter named latch is utilized to avoid rapid control mode switching in the boundaries of the SOC ranges, shown as gray-colored areas in Figure 7a. The control rules in both SS1 and SS2 are determined considering the imbalance between the load and renewable shown in Equation (1), alongside the limits of all assets of MG, which are given in Tables 1 and 3. Moreover, the prioritized load management strategy is designed and utilized in the SS2 dispatch function.

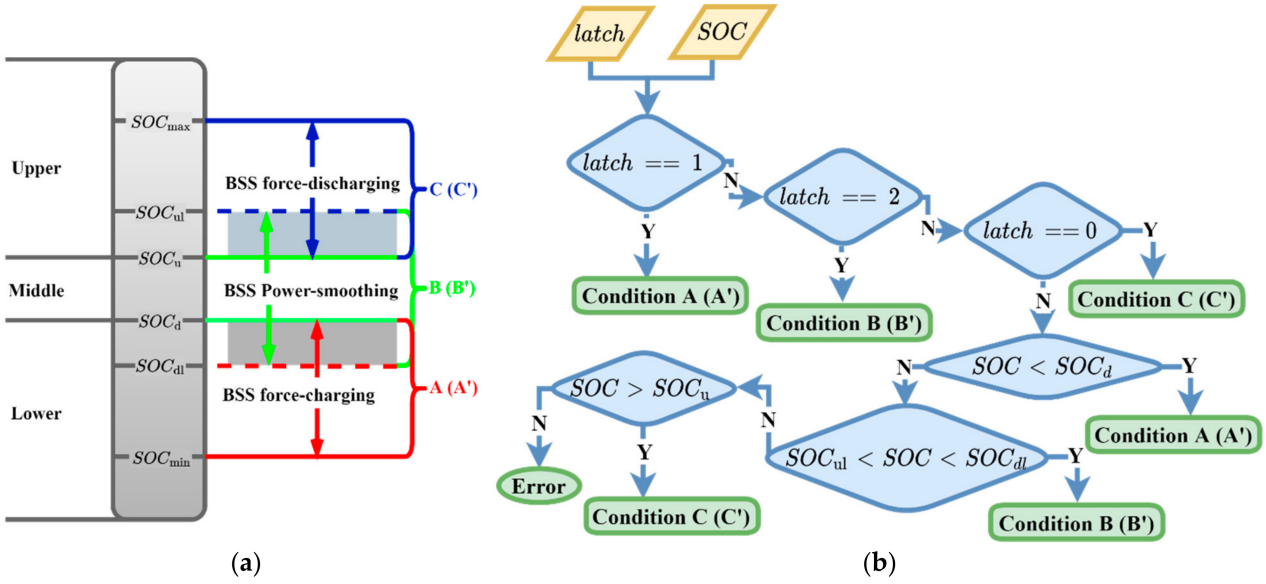

Figure 7. Control modes considering SOC ranges: (**a**) SOC ranges [26]. (**b**) Control mode allocation algorithm.

Table 3. Parameter related to the load management strategy.

Parameter	Description	Parameter	Description
P_{ld}^{tot}	Total load [W] $P_{ld}^{tot} = P_{crt} + P_{Dsh2} + P_{Dsh1} + \sum_{i=1}^{N_{C2}} P_{C2}^{i} + \sum_{i=1}^{N_{C1}} P_{C1}^{i}$	$P_{ld}^{sh,\,tot}$	Total sheddable load (W) $P_{ld}^{sh,tot} = P_{sh1} + P_{sh2}$
P_{C1}^{i}	i^{th} interruptible CCL (W)	P_{C2}^{i}	i^{th} priority CCL (W)
P_{D1}^{i}	i^{th} interruptible DCL (W)	P_{D2}^{i}	i^{th} priority DCL (W)
P_{Csh1}	Total sheddable interruptible CCL (W) $P_{Csh1} = \sum_{i=1}^{N_{C1}} \left(P_{C1}^{i} - P_{C1}^{min,i} \right)$	P_{Csh2}	Total sheddable priority CCL (W) $P_{Csh2} = \sum_{i=1}^{N_{C2}} \left(P_{C2}^{i} - P_{C2}^{min,i} \right)$
P_{Dsh1}	Total sheddable interruptible DCL (W) $P_{Dsh1} = \sum_{i=1}^{N_{D1}} S_{D1}^{i} \cdot P_{D1}^{i}$	P_{Dh2}	Total sheddable priority DCL (W) $P_{Dh2} = \sum_{i=1}^{N_{D2}} S_{D2}^{i} \cdot P_{D2}^{i}$
P_{sh1}	Total sheddable interruptible load (W) $P_{csh1} = P_{Dsh1} + P_{Csh1}$	P_{sh2}	Total sheddable priority load (W) $P_{csh2} = P_{Dsh2} + P_{Csh2}$
$P_{ld,C2}^{res}$	Total restorable priority CCL (W) $\mathrm{P}_{\mathrm{ld,C2}}^{\mathrm{res}} = \sum_{\mathrm{i=1}}^{\mathrm{N_{C2}}} \left(\mathrm{P}_{\mathrm{C2}}^{\mathrm{max,i}} - \mathrm{P}_{\mathrm{C2}}^{\mathrm{i}} \right)$	$P_{ld,C1}^{res}$	Total restorable interruptible CCL (W) $P_{ld,C1}^{res} = \sum_{i=1}^{N_{C1}} \left(P_{C1}^{max,i} - P_{C1}^{i} \right)$
$P_{ld,D2}^{res}$	Total restorable interruptible DCL (W) $P_{ld,D2}^{res} = \sum_{i=1}^{N_{D2}} \left(\left(1 - S_{D2}^{i} \right) \cdot P_{D2}^{i} \right)$	$P_{ld,D1}^{res}$	Total restorable interruptible DCL (W) $P_{ld,D1}^{res} = \sum_{i=1}^{N_{D1}} \left(\left(1 - S_{D1}^{i} \right) \cdot P_{D1}^{i} \right)$
N_{D1}	Number of interruptible DCL	S_{D}^{i}	ON/OFF status of i^{th} DCL
N_{C1}	Number of interruptible CCL	$S_{D}^{spt,i}$	ON/OFF status command for i^{th} DCL (W)

Table 3. *Cont.*

Parameter	Description	Parameter	Description
N_{D2}	Number of priority DCL	$P_C^{spt,i}$	Power setpoint for i^{th} CCL (W)
N_{C2}	Number of priority CCL	$P_C^{min,i}$	Minimum power of i^{th} CCL (W)

The dispatch rules associated with SS2 dispatch mode are illustrated in Figure 8. The commands of dispatch rules will be cited by corresponding, blue-colored labels in Figure 8. In these dispatch rules, the first priority is to define the power setpoint of BSS regarding the SOC ranges, which makes BSS avoid discharge and charge in force-charging and force-discharging conditions, respectively. The second priority is to avoid renewable curtailment and load shedding.

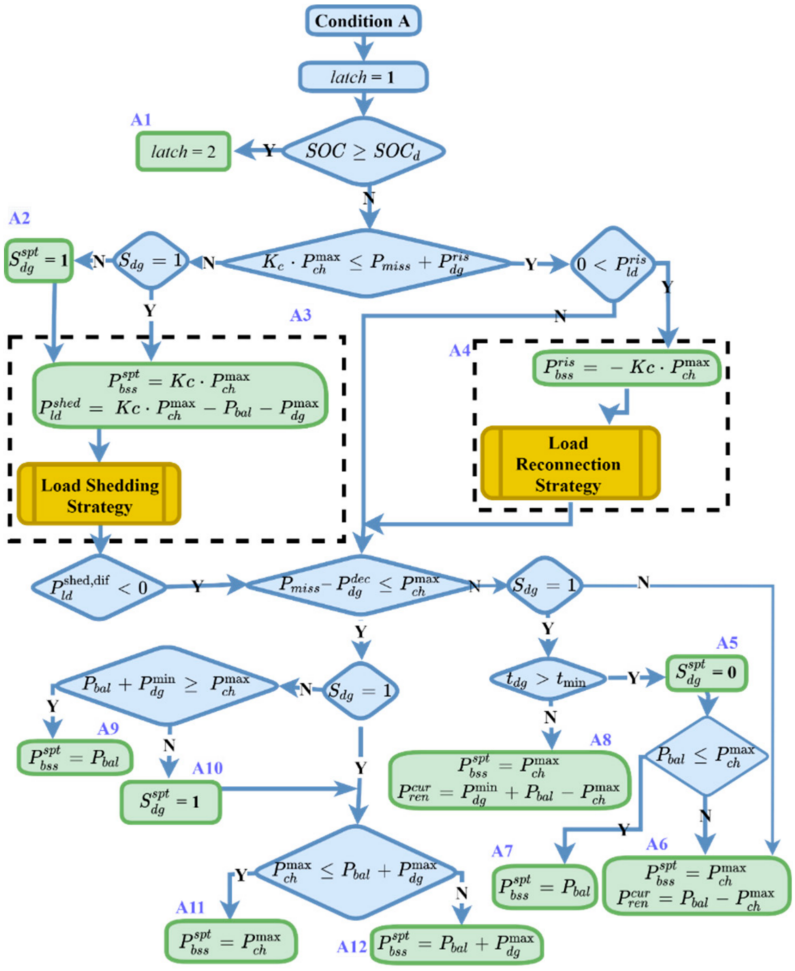

(**a**)

Figure 8. *Cont.*

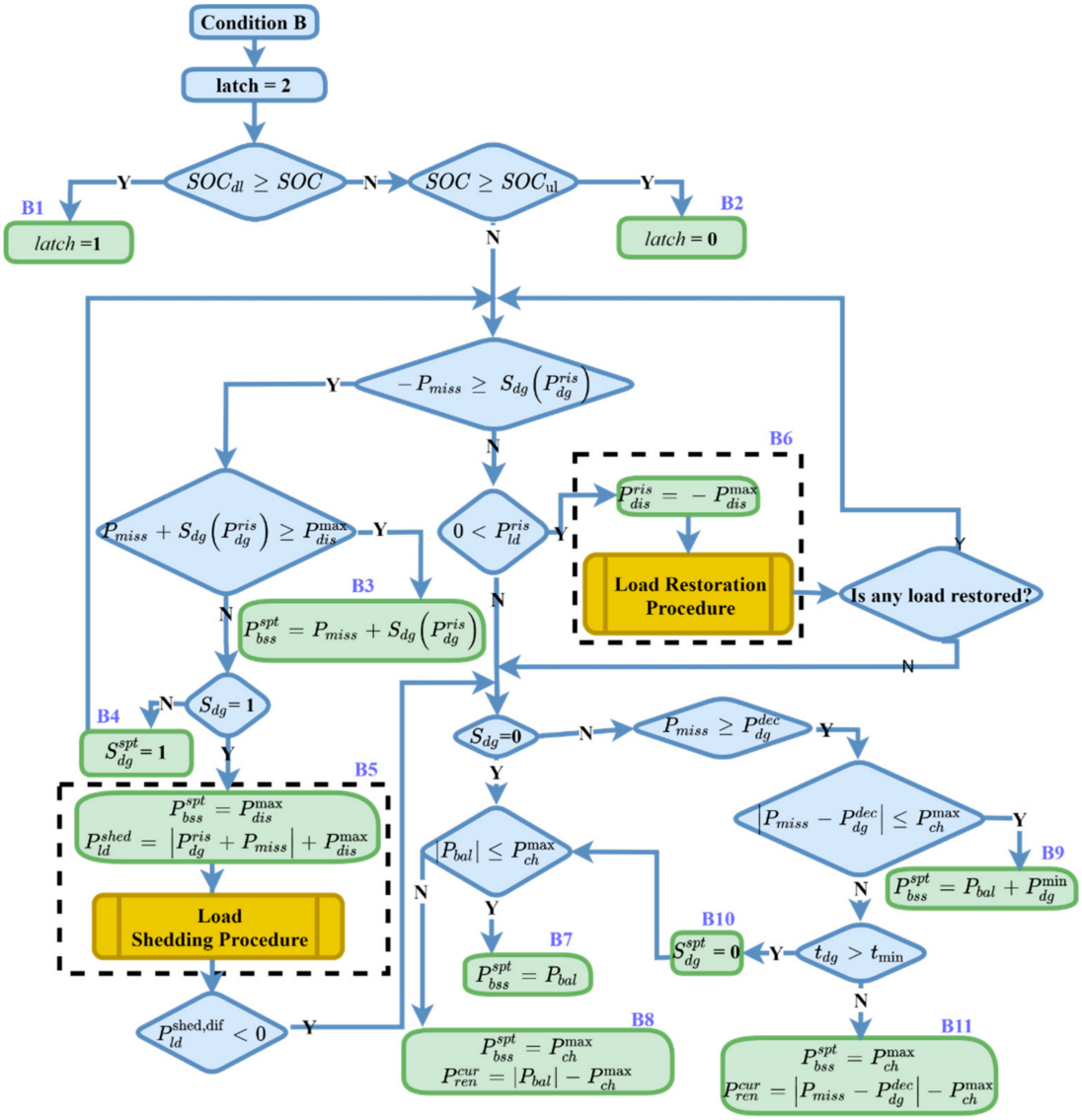

(**b**)

Figure 8. *Cont.*

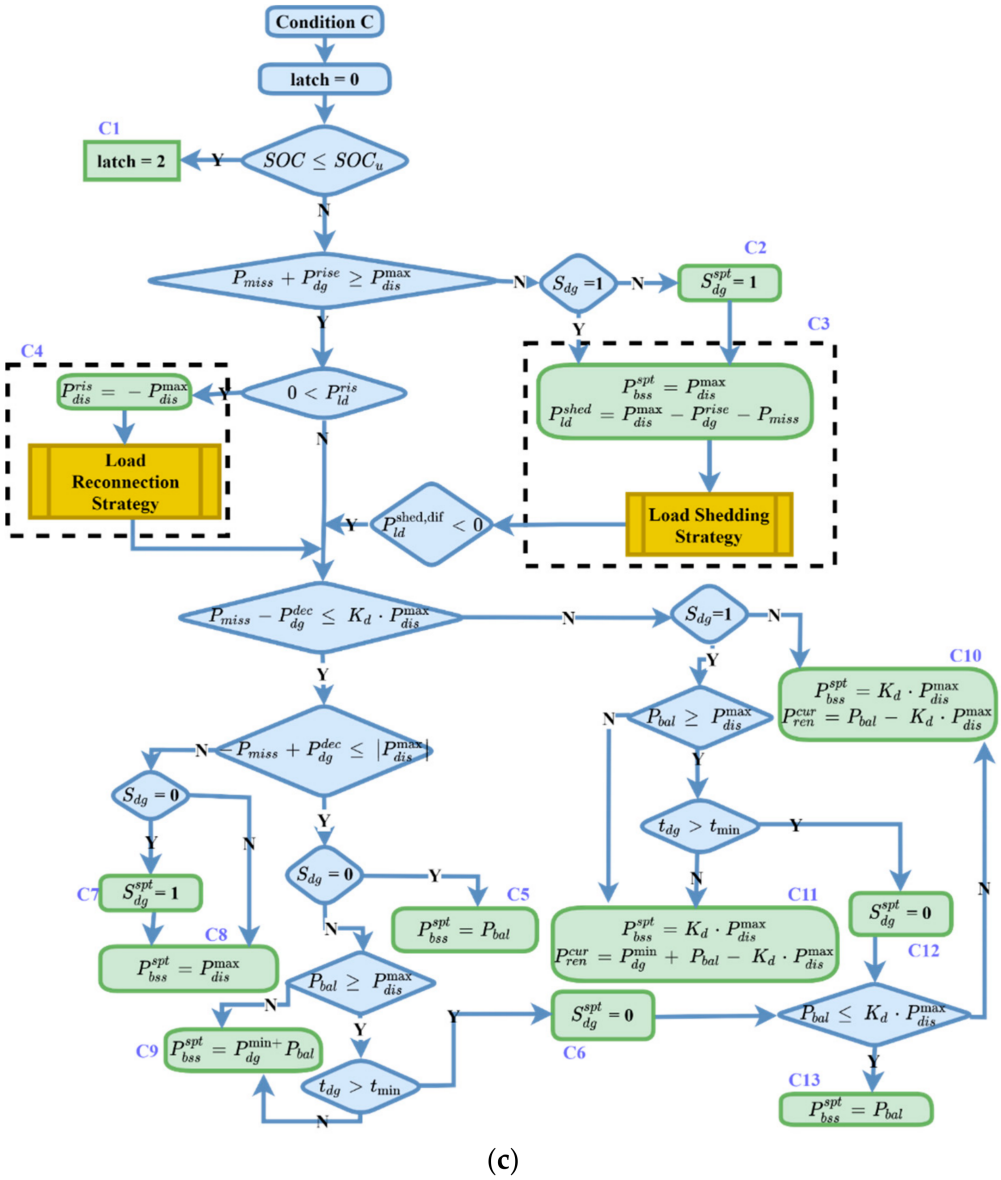

(**c**)

Figure 8. Control rules of dispatch function in SS2 based on the ranges of BSS's SOC: (**a**) BSS force-charging control rule. (**b**) BSS power-smoothing control rule. (**c**) BSS force-discharge control rule.

For the force-charging rule, given in Figure 8a, the allowed operational interval of BSS and DG are given in Equations (2) and (3). Considering these intervals, Equation (5) is derived. This interval indicates the upper and lower limits of P_{miss}, in which load shedding or renewable curtailment is not necessary. P_{miss} is the power mismatch between the generation and load, which is to be compensated by the BSS. In the case of P_{miss} being less than the lower boundary of Equation (5), the operational status of DG has checked whether it is ON. If the DG is OFF, it will be turned ON (A2), then the BSS charging power will be minimum. The required amount of load to be shedded (P_{ld}^{shed}) will then be determined (A3), and the OFF/ON command of the DCLs and CCL's setpoints is determined through the load shedding procedure. Because of the discretely controlled loads, the shedded load might be more than the required amount, which will be checked by $P_{ld}^{shed,diff}$. If this variable is equal to zero, the process will be terminated; otherwise, this difference will be compensated by charging BSS or renewable curtailment.

$$P_{bal} = P_{ren} - P_{ld}^{tot} = P_{miss} - P_{dg} \quad (1)$$

$$K_c \times P_{ch}^{max} \leq P_{miss} \leq P_{ch}^{max} \tag{2}$$

$$P_{dg}^{min} \leq P_{dg} \leq P_{dg}^{max} \tag{3}$$

$$K_c \times P_{ch}^{max} - P_{dg}^{max} \leq P_{bal} \leq P_{ch}^{max} - P_{dg}^{min} \tag{4}$$

$$K_c \times P_{ch}^{max} - P_{dg}^{ris} \leq P_{miss} \leq P_{ch}^{max} + P_{dg}^{dec} \tag{5}$$

where:

$$P_{dg}^{ris} = P_{dg}^{max} - P_{dg} \tag{6}$$

$$P_{dg}^{dec} = P_{dg} - P_{dg}^{min} * S_{dg} \tag{7}$$

If the P_{miss} satisfies the lower boundary interval presented in Equation (5), and the restorable load (P_{ld}^{ris}), given in Equation (8), is available, the load restoration procedure (A5) is executed to update the power and status set point of the loads. Additional to the generation and load imbalance, the possible BSS's share (P_{bss}^{ris}) in the incremental load ($\mathrm{P_{ld}^{incr}}$) is $-K_c \times P_{ch}^{max}$ for this dispatch rule. This means that the minimum BSS charging power is reduced from the incremental load.

$$P_{ld}^{ris} = \sum_{i=1}^{N_{D1}} \left(\left(1 - S_{D1}^{i}\right) \cdot P_{D1}^{i} \right) + \sum_{i=1}^{N_{D2}} \left(\left(1 - S_{D2}^{i}\right) \cdot P_{D2}^{i} \right) + \sum_{i=1}^{N_{C1}} \left(P_{C1}^{max,i} - P_{C1}^{i} \right) + \sum_{i=1}^{N_{C2}} \left(P_{C2}^{max,i} - P_{C2}^{i} \right) \tag{8}$$

Following this, the execution of each of the load management strategy procedures, P_{miss} and P_{bal} values, are updated. The upper boundary interval given in Equation (5) is then checked. If this condition is fulfilled, considering the status and operational limitation of DG, BSS is charged as much as possible (A9, A11, and A12). DG is turned ON (A10) if it is necessary to fulfill this aim. However, if P_{miss} exceeds the upper boundary of the interval, renewables are needed to be curtailed, and BSS power setpoint is P_{ch}^{max} (A6, and A8). The DG might be turned OFF (A5), considering t_{dg} and t_{min} to avoid (A7) or reduce the renewable curtailment.

In dispatch rule B, shown in Figure 8b, the average BSS power is zero, and DG power variations alongside (B3, B7, and B9) with DG status switching will balance the generation and load (B4 and B10). However, BSS and DG might not be able to compensate for the imbalance. Therefore, the load shedding (B5) procedure or renewable curtailment (B8 and B10) will be applied. As in dispatch rule A, the load restoration procedure (B6) can be utilized depending on the assets' operational conditions. For this rule, P_{bss}^{ris} is equal to P_{dis}^{max}, which does not mean BSS will discharge at the maximum rate, and P_{bss}^{spt} is determined in the further steps.

Similar to dispatch rule A, the force-discharging rule can be derived by applying interval analyses to Equations (1), (2) and (9) and reveals the interval given in Equation (10). If P_{miss} does not satisfy the lower or upper boundaries of the interval presented in Equation (10), load shedding (C3), and renewable curtailment (C10 and C11) will be obtained and P_{bss}^{spt} will be set to discharge as much as possible (C5, C8, C9, and C13). However, DG might be turned ON (C2) or OFF (C12), considering t_{dg} and t_{min} to reduce load shedding and renewable curtailment, respectively. The main priority of this dispatch rule is to discharge the BSS; P_{bss}^{ris} is set to be P_{dis}^{max} for load restoration (C4).

$$P_{dis}^{max} \leq P_{miss} \leq K_d \times P_{dis}^{max} \tag{9}$$

$$P_{dis}^{max} - P_{dg}^{ris} \leq P_{miss} \leq K_d \times P_{dis}^{max} + P_{dg}^{dec} \tag{10}$$

The dispatch rules for SS1 dispatch mode (A′, B′, and C′) are illustrated in Figure 9. The main differences between these sets of rules and the previous set are that DG is kept OFF, and instead of load shedding, renewable curtailment, or load restoration, POI active power requirement (P_{POI}^{set}) is updated. For this purpose, Equation (1) has been modified

to Equation (11), and Equations (12) and (13), corresponding to A′ and C,′ respectively, are derived.

$$P^{*}_{bal} = P_{ren} - P^{tot}_{ld} + P^{set}_{POI} \tag{11}$$

$$K_c \times P^{max}_{ch} \leq P^{*}_{bal} \leq P^{max}_{ch} \tag{12}$$

$$P^{max}_{dis} \leq P^{*}_{bal} \leq K_d \times P^{max}_{dis} \tag{13}$$

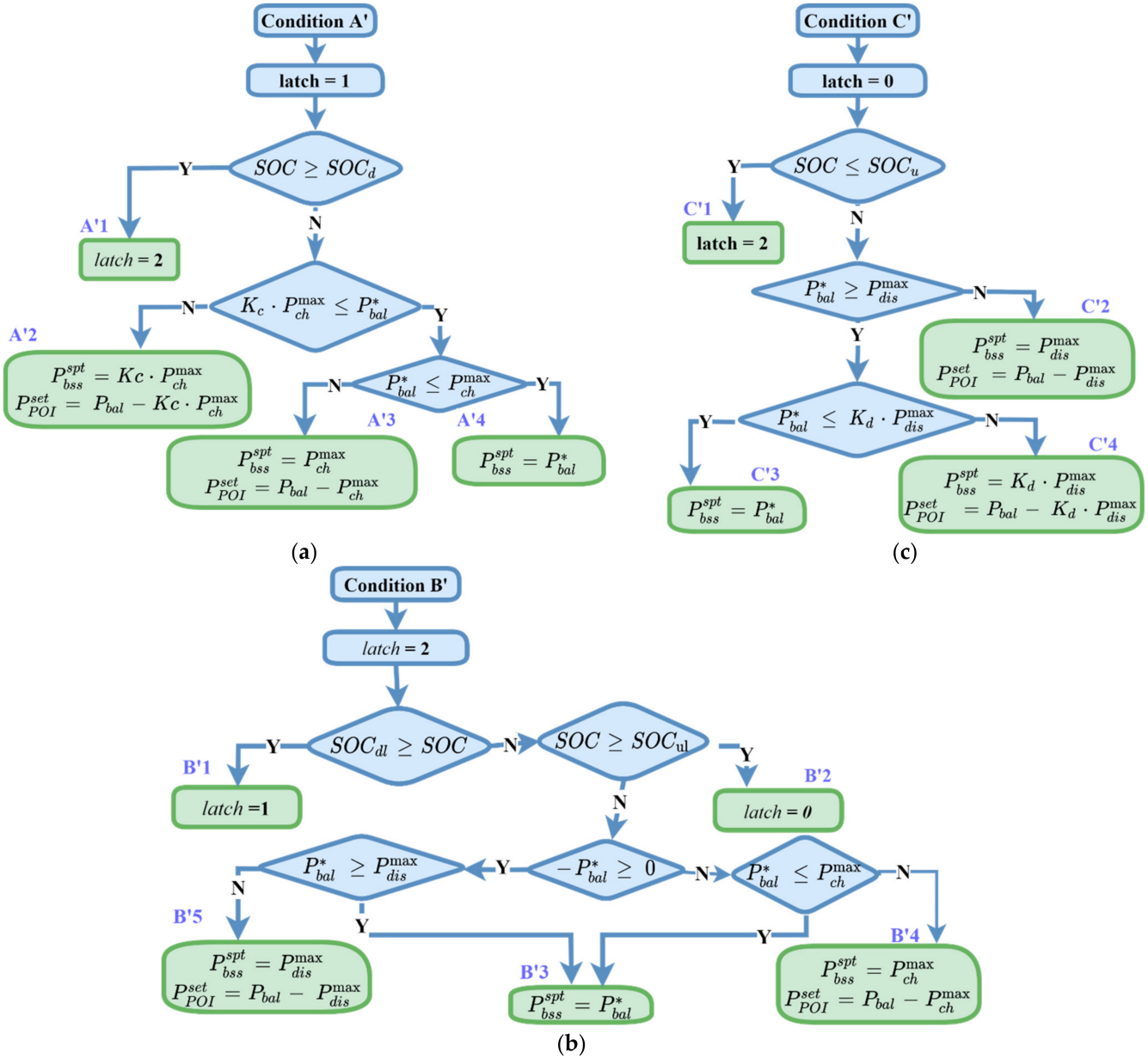

Figure 9. Control rules of dispatch function in SS1 based on the ranges of BSS′ SOC: (**a**) BSS force-charging control rule. (**b**) BSS power-smoothing control rule. (**c**) BSS force-discharge control rule.

3.2.1. Load Management Strategy

Load management strategy consists of two procedures, which are load shedding and load restoration. Both of these procedures are designed regarding the criticality and controllability of loads. Increment or decrement in load might be due to the fluctuations of the renewable resources. Thus, modification is applied first on the CCLs of the considered load category to reduce the ON/OFF actions impacts. Corresponding flow charts to these procedures are presented in Figures 10 and 11, and details of related parameters are

explained in Table 3. It should be noted that the load management strategy is designed to be flexible, and the presence of any kind of load is not necessary for this strategy.

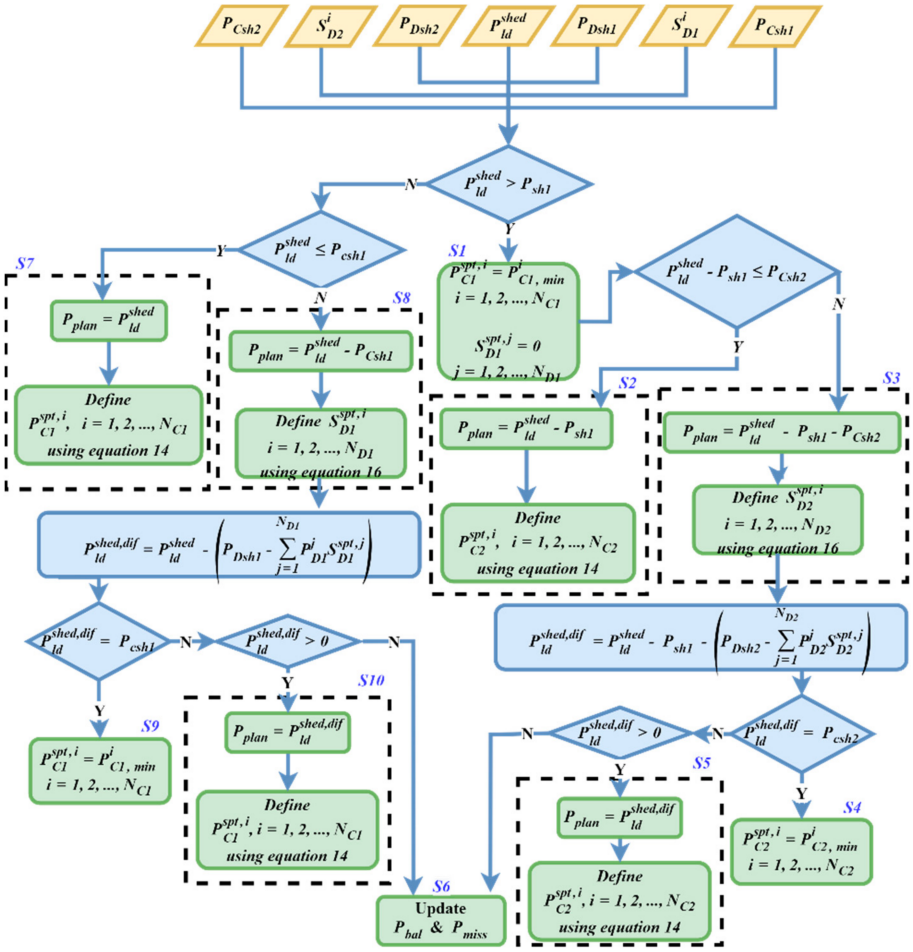

Figure 10. Flow chart of the load shedding procedure.

In these procedures, the weighing methods given in (14) and (15) and the queuing methods given in (16) are utilized to determine setpoints for CCLs and DCLs, respectively. Equation (16) is an optimization problem aiming to determine the ON/OFF status commands for DCLs such that the total power of that set load becomes less or equal to the desired value with the difference minimum difference. This optimization is utilized for both load shedding and restoration procedures. P_{plan} is positive for load shedding and is negative for restoration. Accordingly, the total shedded DCL might be more than the required amount. Therefore, in the case of partially shedding both CCL and DCL, it is first supposed that all CCL is shedded (S3 and S8 in Figure 10). If the resultant shedded DCL is less than the desired, the mismatch is compensated by CCL (S5 and S10 in Figure 10). In the restoration procedure, a similar logic compared to the load shedding is obtained. Similarly, the CCL loads is considered in this algorithm to avoid rapid load switching due to renewable intermittency. However, the priority load group is restored first.

$$w_i = \frac{P^i_C - P^{min,i}_C}{\sum_{i=1}^{N_C}\left(P^i_C - P^{min,i}_C\right)} P^{spt,i}_c = P_C - w_i \cdot P_{plan} \tag{14}$$

$$w_i = \frac{P^{max,i}_C - P^i_C}{\sum_{i=1}^{N_C}\left(P^{max,i}_C - P^i_C\right)} P^{spt,i}_c = P_C + w_i \cdot P_{plan} \tag{15}$$

$$\max \sum_{i=1}^{N_D} S_D^{spt,i} \cdot P_{D2}^i \text{Such that : } \sum_{i=1}^{N_D} S_D^{spt,i} \cdot P_{D2}^i \leq -P_{plan} + \sum_{i=1}^{N_D} S_D^i \cdot P_{D2}^i \quad (16)$$

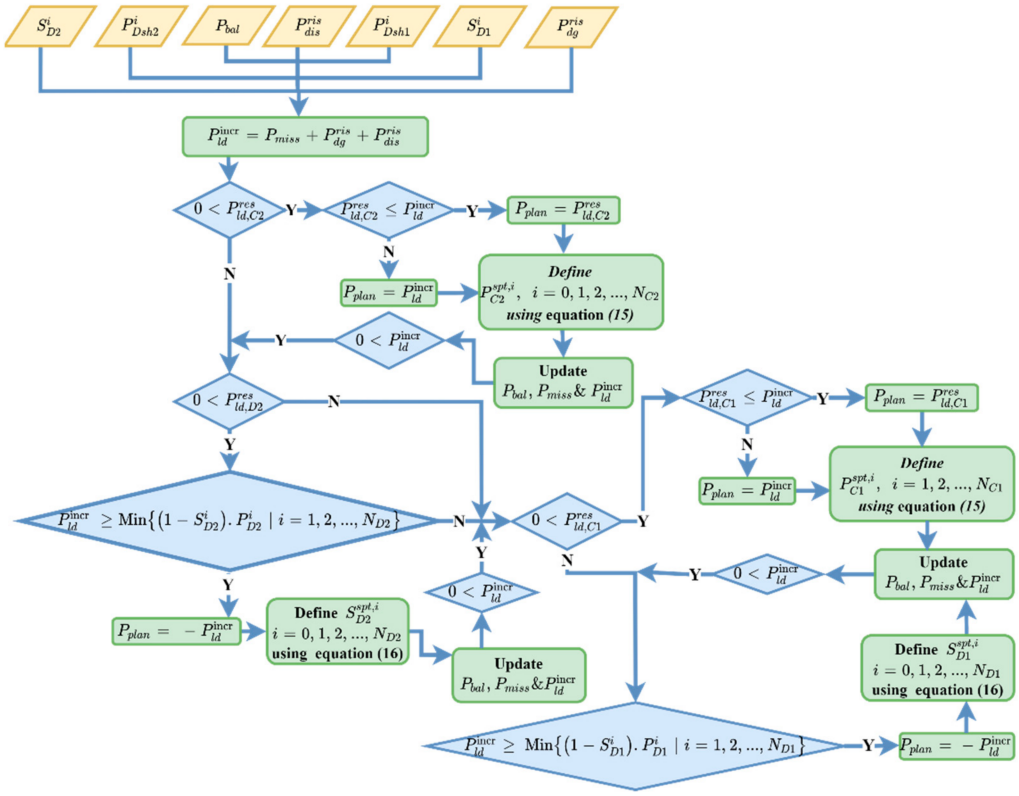

Figure 11. Flow chart of the load restoration procedure.

3.2.2. The Emergency Dispatch Order (EDO)

There is an exception for dispatching the MG assets. When the unplanned islanding event is detected, EDO will be executed directly by the transition function. Unplanned islanding, unlike planned islanding, makes it impossible to alter the DER controller set point or operating point in real-time. Because of the low inertia of power electronic converters, the voltage and current output of DER may experience substantial deviations in this circumstance. Therefore, this order is continuously updated as conditions change, and MG status is updated and is available for execution without waiting to be computed. The calculation process of this rule is shown in Figure 12. DG is off during SS1, and grid forming will be performed via BSS during SS2. Therefore, depending on the MG status, DG is turned on via EDO (E5). The presence of DG is not counted in load shedding (E4) because of the limited response speed of diesel generators.

3.3. The Transition Function

The transition function contains the logic for shifting the dispatch function between one of the essential dispatch modes to prevent or to delay a disconnection in a way that violates the interconnection requirement. In the recent approach, the transition function consists of planned and unplanned islanding transitions. The determined dispatch mode is fed to the dispatch function, and the dispatch function applies the dispatch based on this. However, during T1 and T2, the dispatch orders are executed by the transition function, and the dispatch mode returns to SS1 or SS2. In both T1 and T1, the POI CB will be opened, and BSS control will be shifted to *Vf* control mode by the transition function. The flowchart corresponding to this function is presented in Figure 13.

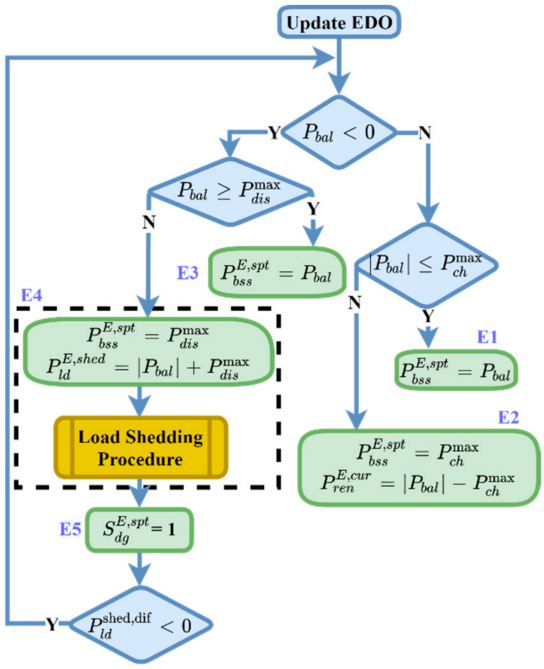

Figure 12. Emergency dispatch order calculation flowchart.

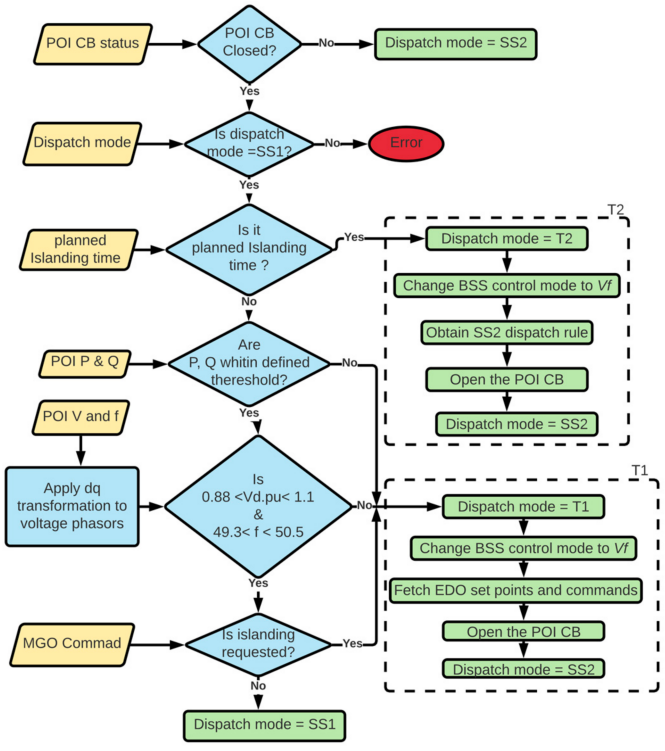

Figure 13. Transition function including T1 and T2.

The first step in this procedure is to check the status of POI's CB. The planned islanding transition requirement is then assessed. This process began to be obtained t_{isld} seconds before the planned time. t_{isld} is an adjustable variable depending on the response speed of the MG's assets. As the planned event is detected, the transition function will determine the assets' setpoints based on SS2 dispatch rules, and algorithms are given in Figures 7b and 8.

In this manner, the exchanged power at POI will be set at zero by implementing essential load shedding or renewable curtailment. Then dispatch mode will switch to SS2.

$$V_d = -\frac{2}{3}\{[V_a \cdot \cos(2\pi ft) + V_b \cdot \cos(2\pi ft + 2\pi/3) + V_c \cdot \cos(2\pi ft - 2\pi/3))\} \quad (17)$$

The MG remains connected to the grid if required criteria by DSO or MGO are satisfied [21]; otherwise, MG will be islanded. In this approach, unplanned islanding is achieved by monitoring the total active power, frequency, and voltage at the POI. However, instead of three-phase voltage, V_d [29,30] should be within the specified interval. V_d is calculated based on Equation (17), where V_a, V_b, V_c, and f are phase voltages and MG nominal frequency, respectively. In addition, unplanned islanding events could be initiated by an external or internal command from DSO or MGO. If any of the mentioned conditions are satisfied, an unplanned islanding event will take place. In this regard, the calculated EDO will be executed by the transition function immediately, then the rest of the required actions stated will be performed.

4. Test Results

In this section, the test results are presented. The considered system is presented in Figure 2, in which the positive directions of power flows are illustrated. Noncritical loads consist of both continuously and discretely controllable ones. The tests are based on the actual setup at the Middle East Technical University. The parameters related to the considered system are presented in Table 4.

Table 4. Parameters of the considered system for tests.

Parameter	Value	Parameter	Value
$t_{\min}$	600 s	BSS energy capacity	350 kWh
P_{dg}^{min}	2 kW	SOC_{min}	20%
P_{dg}^{max}	50 kW	SOC_{max}	90%
P_{ch}^{max}	10 kW	SOC_{dl}	35%
P_{dis}^{max}	−10 kW	SOC_{d}	40%
K_c	0.05	SOC_{u}	60%
K_d	0.05	SOC_{ul}	65%
N_{D1}	5	N_{D2}	3
N_{C1}	4	N_{C2}	3
$P_{C1}^{min,i}$	1, 1.5, 1.2, 0.5 kW	$P_{C2}^{min,i}$	1.5, 1, 1.4 kW
$P_{C1}^{max,i}$	8, 2.5, 6, 5 kW	$P_{C2}^{max,i}$	8, 6, 8.5 kW

The primary purpose of forming cases is to cover all dispatch rules in both dispatch modes in various conditions. The IEEE 2030.8 standard [22] specifies tests to test the pertinent operation of the dispatch function. In this regard, three test cases are formed, and details related to the assets for each case are given in Table 5.

- **Case-a:** This case is prepared to investigate the advantage of keeping the BSS around 50%. For this purpose, a dispatch rule regardless of BSS's SOC is utilized in which the determined BSS power can be any value greater and lower than P_{dis}^{max} and P_{ch}^{max}, respectively. The related flowchart of this rule is illustrated in Figure 14. The same system is considered for both methods, and the results are compared. The time step related to this test and the dispatch function is 5 min.
- **Case-b:** In this case, the proposed dispatch function is compared with the dispatch functions presented by Sun et al. in [25], in which DG is only turned OFF by initiation of the force-discharging rule, regardless of MG status. The main objective is to show how proper control of the DG can affect the controller's performance during SS2. The initiation SOC is 55%, making both dispatch functions obtain the power-smoothing dispatch rule.

- **Case-c**: In this case, the performance of the dispatch function in normal conditions during SS1 mode is tested. For this purpose, tests cover two sequential days to observe the control mode switching properly. The time step related to this test and the dispatch function is 5 min. The variance of load and renewable generation in the collected dataset is low from sunset to sunrise. Therefore, all tests started at 5 AM. In addition, the initial required P_{POI} was set to −100 kW.
- **Case-d**: In this case, the consequent performance of the dispatch function to the start and stop of the largest load will be assessed. The duration of the test is 6 h, and MG is in islanded mode. The time step related to this test and the dispatch function is 1 min.
- **Case-e:** This case is performed to observe the proper reaction of dispatch function to temporary loss of the PV system during SS2. The duration of the test is 6 h. The time step related to this test and the dispatch function is 1 min.
- **Case-f:** In this case, DG is not connected to the system, where upper and lower boundaries of this are considered to be zero. The time step related to this test and the dispatch function is 5 min.

Table 5. Description of details of test cases.

Case	Initial BSS *SOC*	DG Presence	P_{ren} (kW)		P_{ld}^{crt} (kW)		Noncritical DCL (kW)	
			Average	Max	Average	Max	Average	Max
c	25%	No	84.8	190	21.7	43	46.5	79
d	55%	Yes	106	148.5	37.2	91.1	53.4	105.7
e	70%	Yes	85	148.5	32.3	35.2	84.2	102.2
e	85%	No	85	148.5	21.2	41.3	53.4	105.7

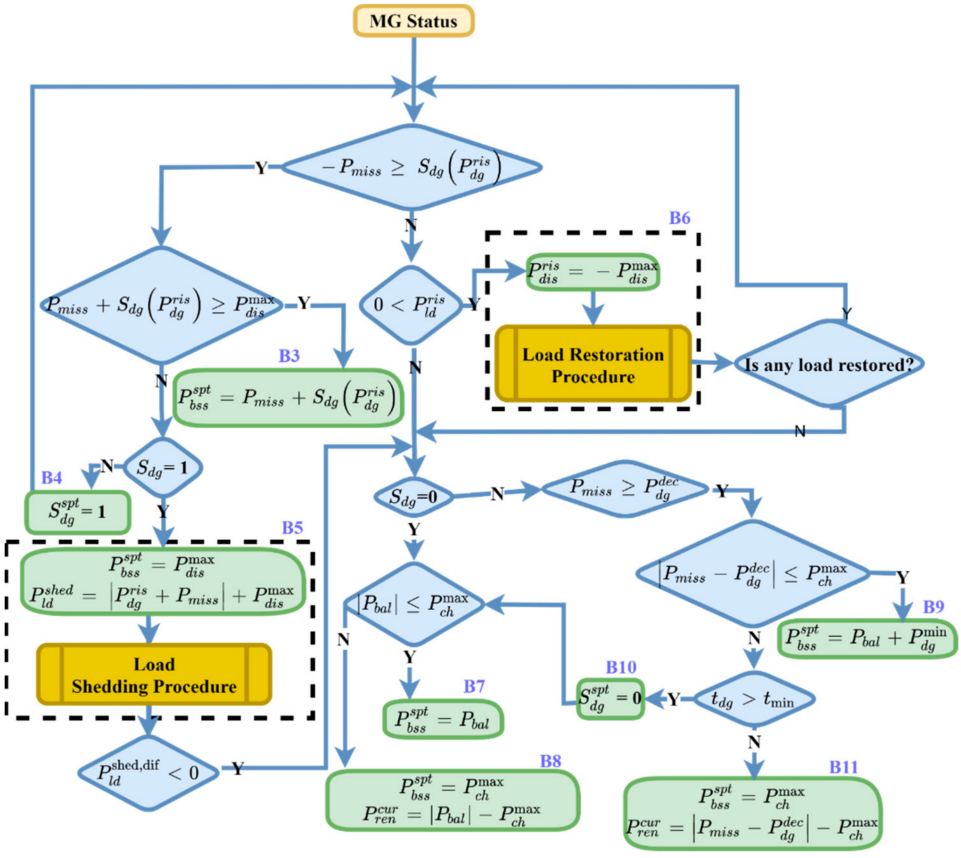

Figure 14. A non-SOC following rule-based dispatch rule.

The test results for Case-a are shown in Figure 15. According to Figure 15a, when dispatch is fulfilled, regardless of SOC, the BSS SOC has decreased to the desired minimum

value. Therefore, BSS is not able to inject any power to the MG, and support of the critical loads is completely dependent on the DG. This situation can cause an unreliable supply of the MG's critical loads such that, in case of DG failure, those loads will be shedded. On the contrary, as can be seen in Figure 15b, the proposed dispatch function maintains to SOC around 50% and avoids continuous discharge of BSS.

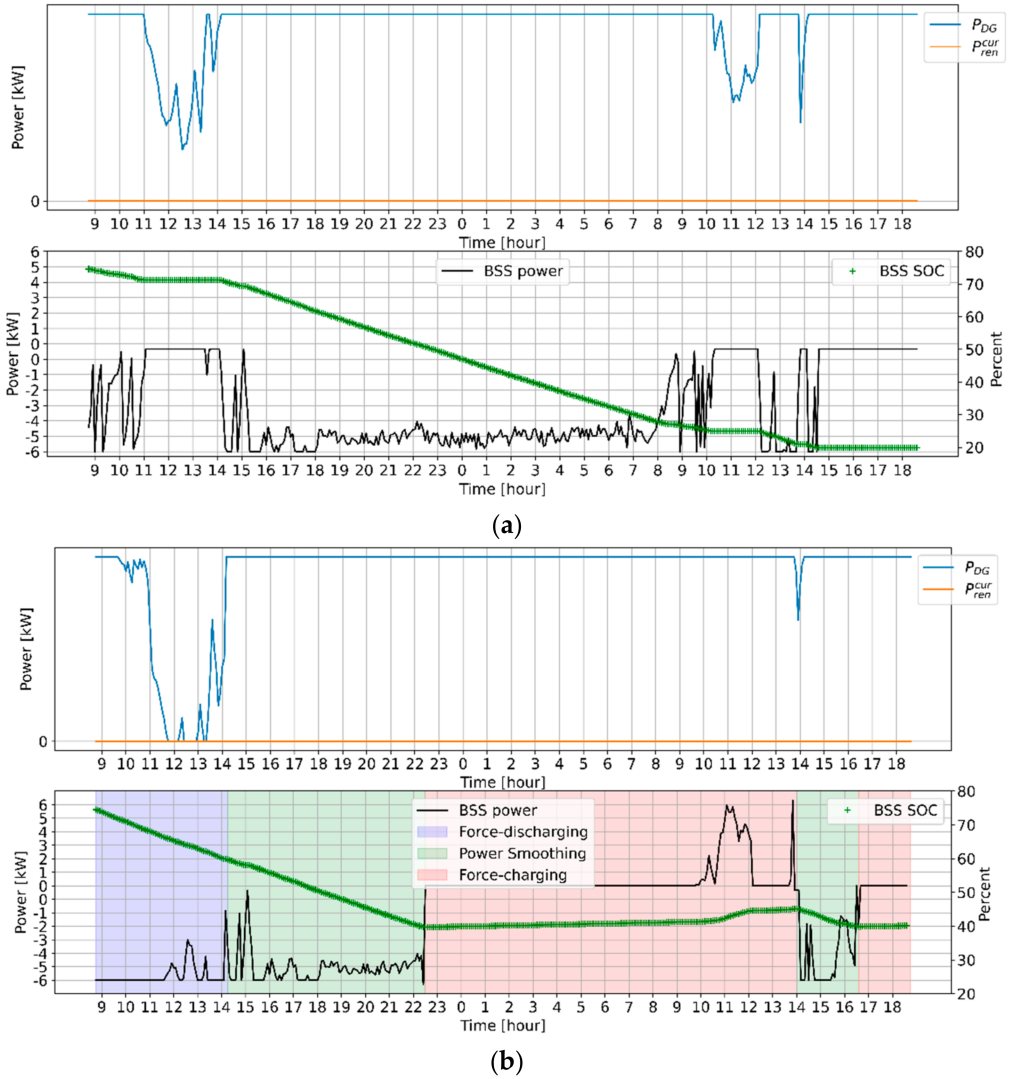

Figure 15. Test results of Case-a: (**a**) MG is dispatched by non-SOC following dispatch rule. (**b**) MG is dispatched by the proposed SOC following dispatch rules.

In Case-b, the performance comparison of the proposed dispatch function (Method 1) and the method of Sun et al. [25] (Method 2) is illustrated in Figure 16. In this Figure, $P1_{DG}$, $P1^{cur}_{ren}$, $P2_{DG}$, and $P2^{cur}_{ren}$ are resultant DG powers of Method 1 and Method 2 and the resultant curtailed renewable power powers of Method 1 and Method 2, respectively. Based on Figure 16a, the generation surpasses the load around 13 for two hours. Accordingly, renewable curtailment is required, and DG power is decreased in both methods. While $P2^{cur}_{ren}$ has been kept at 10 kW, as DG cannot be turned OFF, $P1^{cur}_{ren}$ became 0 as Method 1 has turned DG OFF. In this manner, curtailed renewable power was 10 kW less.

The results of Case-c are illustrated in Figure 17. The initial SOC is 25%, which makes the dispatch rule force-charging. However, the power exchange is less than the set value. Accordingly, BSS power is set to be the minimum charging power tile at sunrise (8 AM). After sunrise, renewable power increases, which increases the P_{POI} up to more than -100 kW. Starting from this point, BSS power increases up to the maximum. As SOC

crosses SOC_d, the control mode is switched to power-smoothing. After 10 PM, SOC enters the force-discharging region. Because of the zero renewable generations and defined dispatch rule, BSS is discharged at the minimum rate. In this test case, both aims are achieved to minimize charge–discharge cycles and avoid rapid control rule switching.

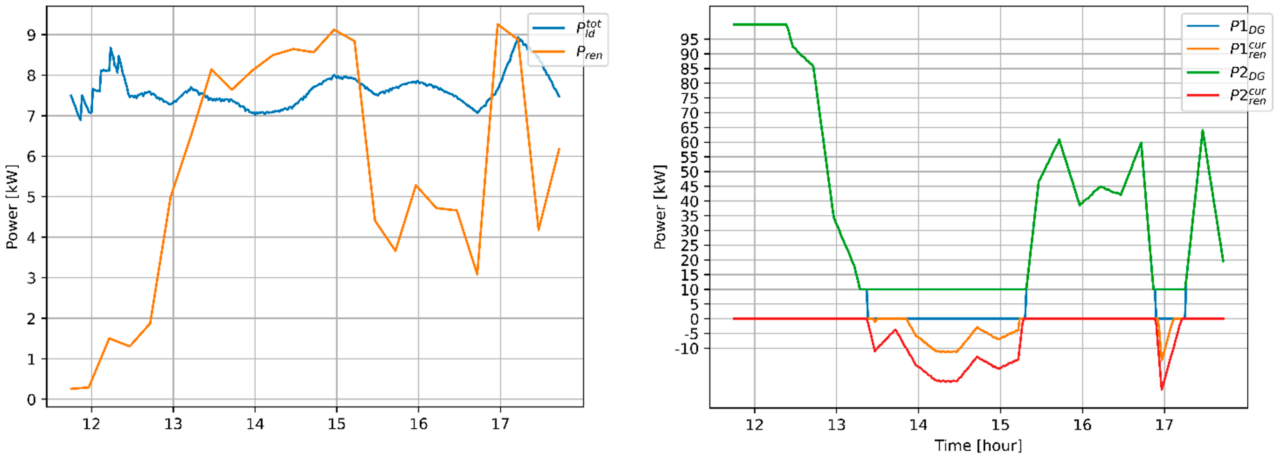

(**a**) (**b**)

Figure 16. Test results of Case-b: (**a**) The load and generation through tests of Case-b. (**b**) Resultant DG power and curtailed renewable power of the proposed dispatch function and the dispatch function developed by Sun et al. in [25].

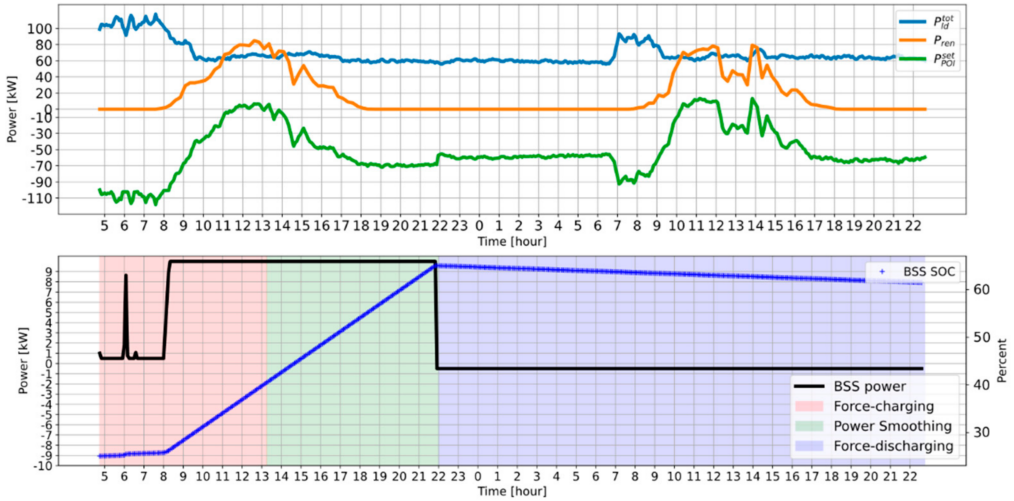

Figure 17. Test results for Case-c: MG in SS1 is tested for two days.

Figure 18 illustrates the test results of Case-d. In this test, a 45 kW load, larger than all other loads, is connected to the system at 11 AM and disconnected 30 min later. This load is considered as the critical load (CL) to avoid its shedding. Based on Figure 18a, the necessary amount of the noncritical load (NCL) is shedded to compensate for the generation and load mismatch immediately after the surge in load. Accordingly, available generation power, BSS discharge power, and load after control (LAC) are balanced. As can be seen in Figure 18c, a single interruptible DCL and both priority and interruptible CCLs are shedded. This means that priority CCLs are shedded instead of shedding extra interruptible DCL. After a couple of minutes, shedded loads are restored as PV power output increases. Moreover, Figure 18b shows, around 30 min before the event, DG power and BSS discharging rate have started decreasing in response to PV power output rise. Precisely after the event, both of these variables are set to corresponding maximums to minimize the shedded load. The SOC remained within the power-smoothing range during

the test. If the dispatch was force-charging before the event or because of the event, the power balance might fail. This issue entirely depends on the sizing of the MG assets and should be contemplated in MG planning.

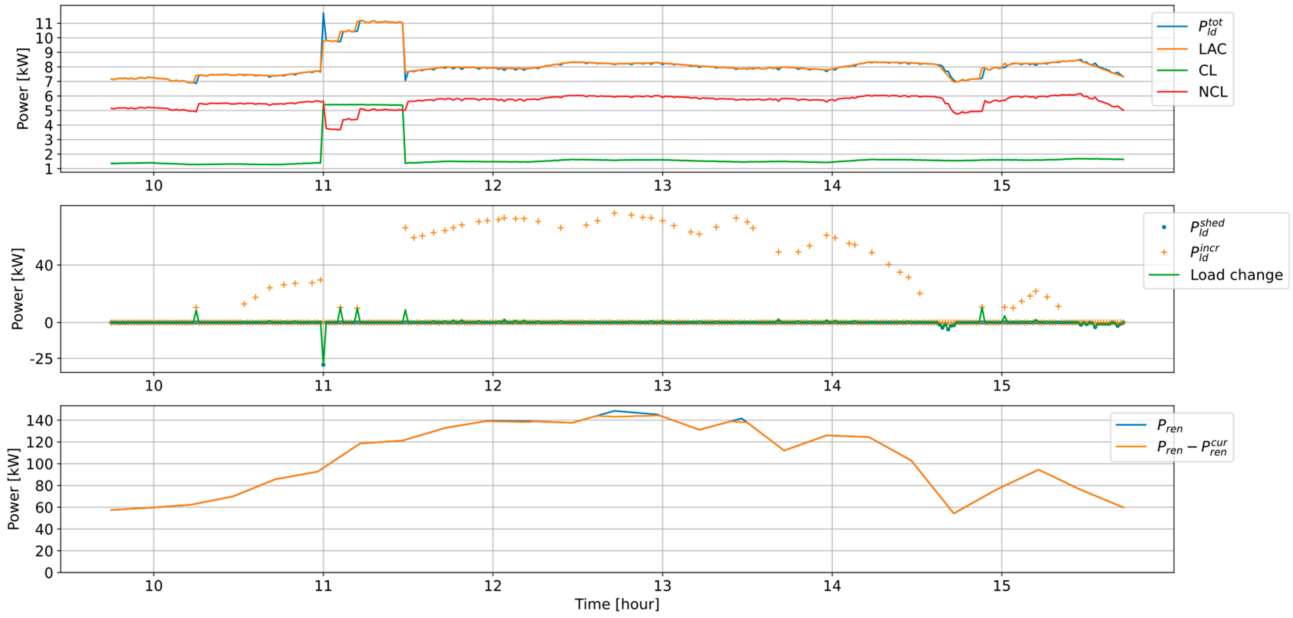

(**a**)

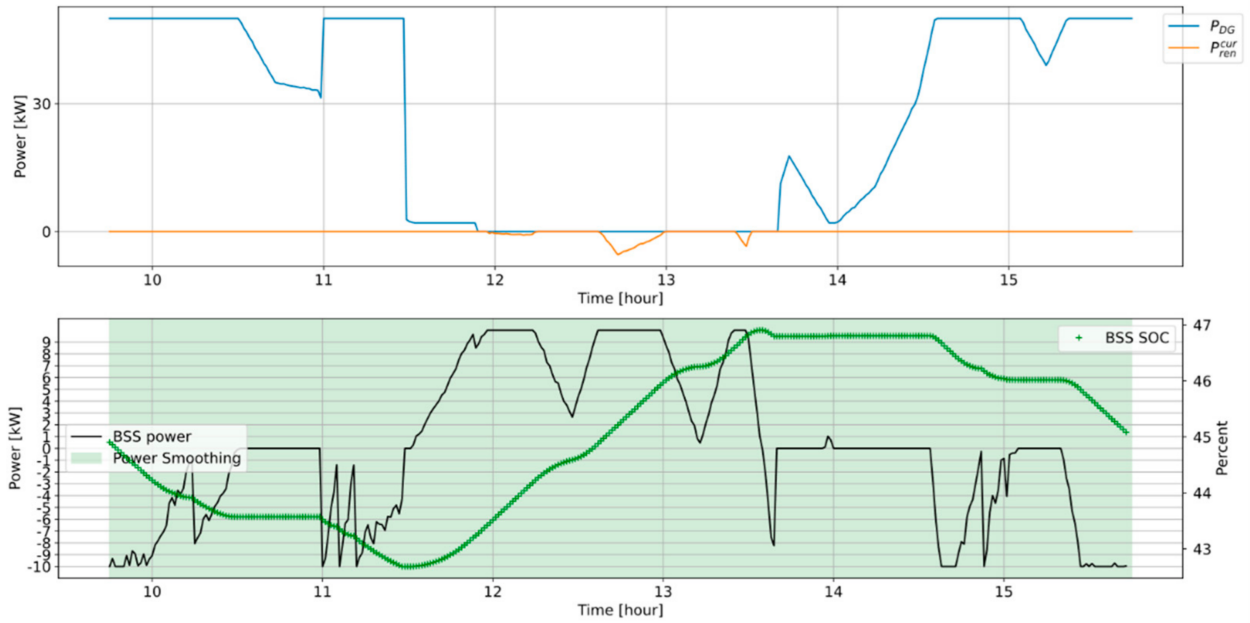

(**b**)

Figure 18. *Cont.*

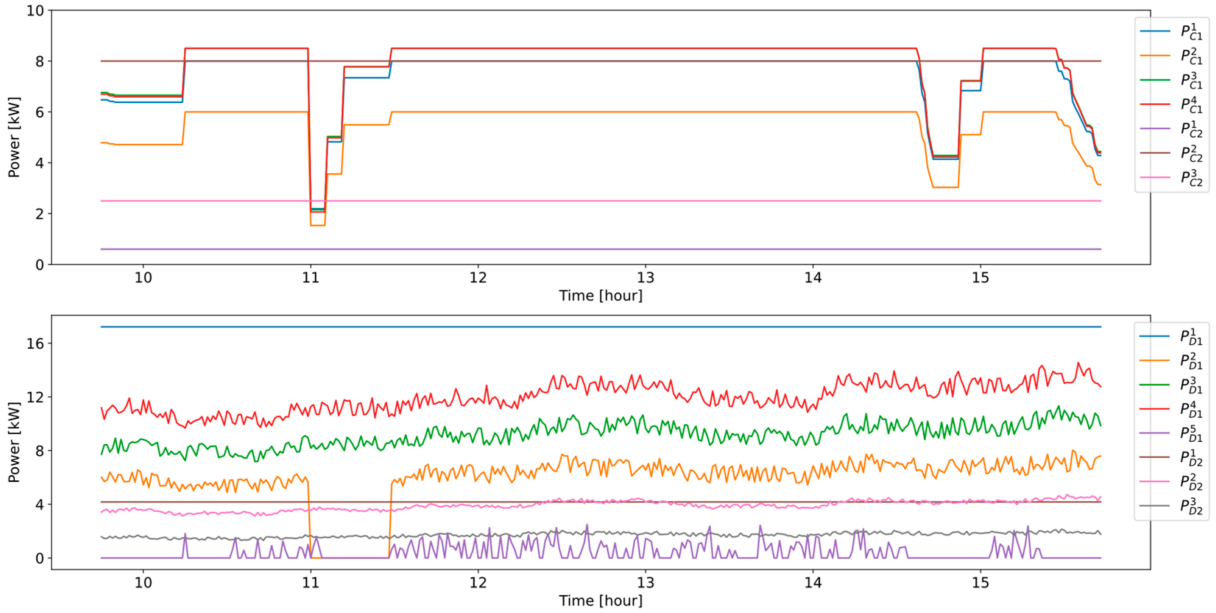

(**c**)

Figure 18. Test results of Case-d: A large load is connected at 11 AM for 30 min. (**a**) Variation of the total load demand and PV generation. (**b**) Variation of the DG power output, curtailed PV generation, BSS SOC, BSS energy, and obtained dispatch rules during the test. (**c**) Illustration of power of individual DCLs and CCLs through the test.

The results of **Case-e** are illustrated in Figure 19. The initial SOC is 70%, indicating dispatch rule force-discharging. The PV system is lost at 1 PM and is returned to the system after one hour. Before this event, the DG is turned off, even renewable generation is partially curtailed, and BSS discharging is at a minimum rate. Immediately after the PV system's tripping, the DG system is turned on and operated at maximum rated power. BSS discharging power increased, and the rest of the power mismatch is compensated by the shedding of NCL. Figure 19c shows that interruptible DCLs and CCLs are shedded entirely. CCLs are then minorly restored during the event in response to priority DCL and CL's variances. After the event ends, DG has turned off again, and BSS power is decreased.

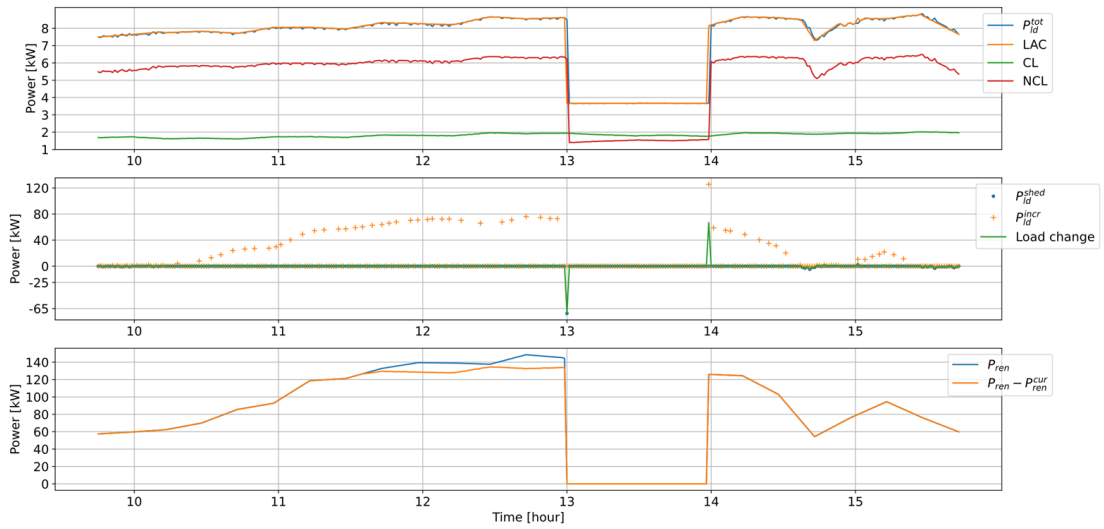

(**a**)

Figure 19. *Cont.*

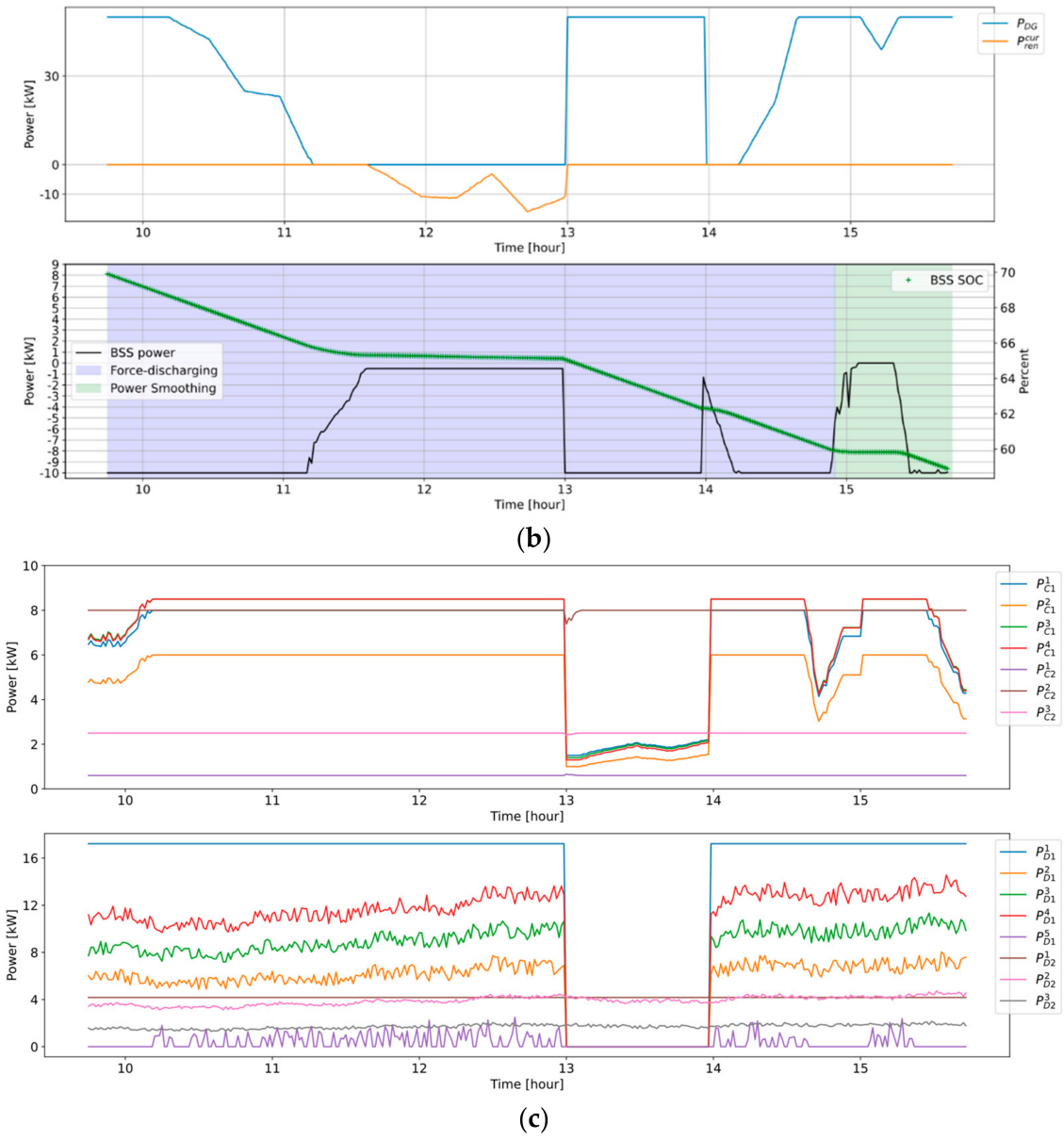

Figure 19. Test results of Case-e: The PV system is tripped at 1 PM for one hour. (**a**) Variation of the total load demand and PV generation. (**b**) Variation of the DG power output, curtailed PV generation, BSS SOC, BSS energy, and obtained dispatch rules during the test. (**c**) Illustration of power of individual DCLs and CCLs through the test.

The test results related to Case-f are given in Figure 20. Within this test, DG is not available and generation is balanced via PV and BSS power. As the BSS is in force-discharging mode, its power output is set to maximum discharging rate up to around 10 AM, where renewable power significantly rises and it is partially curtailed. Meanwhile, all possible loads are restored. However, in the case of a major fall in PV power, load shedding is observed. According to this test, it can be deduced that MGCS can manage the MG without the DG.

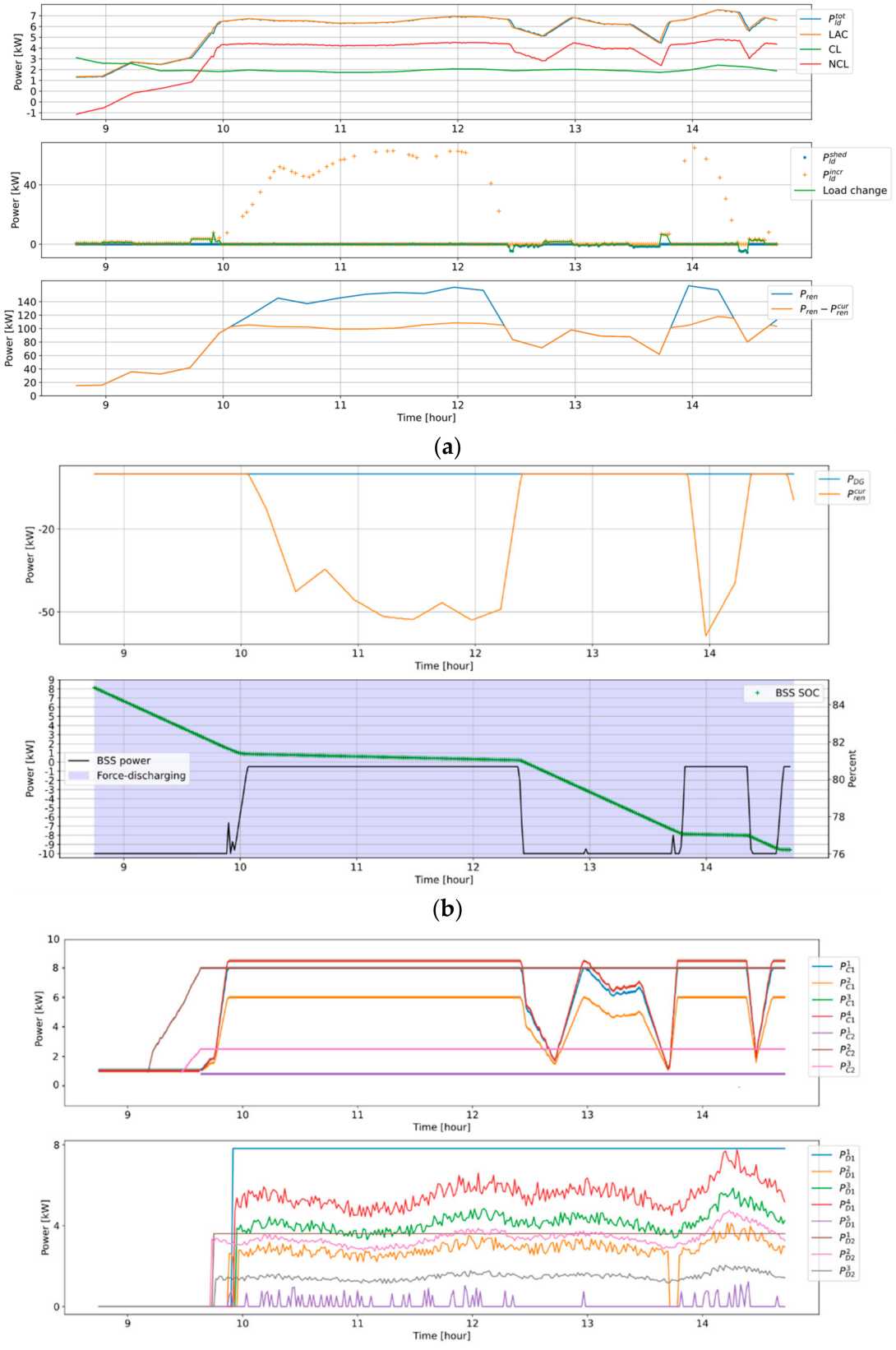

Figure 20. The results of Case-f: The DG is excluded from the system to test the dispatch function being generic. (**a**) Variation of the total load demand and PV generation. (**b**) Variation of the DG power output, curtailed PV generation, BSS SOC, BSS energy, and obtained dispatch rules during the test. (**c**) Illustration of power of individual DCLs and CCLs through the test.

5. Conclusions

This paper develops a field unit (MCCD) designed for real-time centralized MG control. The proposed system presents a complete system solution, including the required hardware and software. The field data is acquired by MCCD from the field and transmitted to the CMTS, where this information is processed and consequent commands are executed. The MCCD can also implement the commands from the CMTS.

The functionalities of the CMTS are compatible with IEEE 2030.7 and 2030.8 standards. The communication framework among these system components is established through a TCP/IP internet socket. MCCD consists of three synchrophasor measurement channels. GPS provides the required time reference single. The CMTS includes four modules to provide autonomous control of MG, online monitoring, data visualization, and manual operations by MGO. The generic MG control functions include dispatch and transition core-level functions. These functions dispatch the MG assets with a BSS SOC-following logic. The primary purpose of this logic is to keep SOC around 50% for the sake of MG resiliency and BSS lifetime. The generic dispatch function is assembled by a load management strategy and dispatch rules that follow SOC. According to both the criticality and the controllability of loads, the load management method sheds and restores the specified amount of load. Because of these control capabilities, the proposed MGCS may be used in various MGs, independent of their size or application. For future works, state estimation can be added to this control and monitoring system to avoid bad data in case of communication failure or MCCD malfunction. Additionally, the higher-level functions mentioned in IEEE 2030.7, such as load and renewable generation forecasts, optimal dispatch, and market participation, can be jointed to core-level functions.

Author Contributions: Conceptualization, M.G. and O.K.; methodology, S.P.-k.; software, S.P.-k.; hardware, M.U. and E.B.; writing—original draft preparation, S.P.-k.; writing—review and editing, M.G.; visualization, S.P.-k.; supervision, M.G. and O.K. project administration, B.C.Ç. All authors have read and agreed to the published version of the manuscript.

Funding: This research was funded by ENERJISA industrial project "Mikro Şebeke Kontrol ve Haberleşme Cihazı Geliştirilmesi Projesi", under project number 376649, and the Scientific and Technological Research Council of Turkey (TUBITAK) under grant number 119E209.

Institutional Review Board Statement: Not applicable.

Information Consent Statement: Not applicable.

Data Availability Statement: Not applicable.

Conflicts of Interest: The authors declare no conflict of interest.

Appendix A

This section gives the description of the design and implementation of the module of the CMTS that has not been explained in Section 2.

Appendix A.1. Database Module

It is necessary for the MGCS to have a database to store the events, execute commands, and measure and process data for future applications. The stored data is accessed and exported through the user interface. The related time scheduling and strategy for this data storage are critical due to storage limitations, and technical considerations are given resolution; therefore, the corresponding resolution is not specified. The data update resolution and storage duration are illustrated in Table A1.

Table A1. The storage strategy in the database module.

Data	Resolution	Storage Duration
Three-phase voltage and current phasor and RMS measurements, frequency, active power, reactive power, apparent power, and power factors	10 Hz 1-s average 1-min average 5-min average 1-h average	24 h One day One month One year Ten years
Forecasts	15 min 1-h average	One year Ten years
Executed commands	-	One year
MCCD status error reports	-	Six months
MGCS error reports	-	Forever
Calendar	Once a year	One year
Academic calendar	Once a year	One year
Weather	Once a min	One year
Network topology and parameters	In case of change	Forever

Appendix A.2. Communication Module

Real-time communication between the MCCD and the MCMS takes place over the Internet network. To enable end-to-end data communication over the Internet, the internet protocol suite (TCP) is used. It specifies all the necessary processes, such as how data should be packaged, addressed, transmitted, forwarded, and received. TCP is used to define how applications create channels to communicate over a network. TCP also allows the arrangement of packet size for messages before they are transmitted. IP is used to address and route individual packets so that they reach the correct destination. Thanks to TCP/IP, data loss is prevented during end-to-end communication, although this functionality may cause some time delays [31]. Therefore, a suitable method for data acquisition should be used in the implementation.

The exchange of data between the different components of MGCS is the main common interface of these components. These messages and corresponding transmission frequency are given in Table A2, where IDBIT and ODBIT stand for initialization device-built-in test and operational device-built-in test, respectively. These messages include the status and related information of modules of MCCD. All the data packages transmitted include sender, receiver, and the data type of the message, the message, and the message ID.

Table A2. Description of messages transmitted between CMTS and MCCD.

Message's Name	Send Frequency
From MCCD to MCMS	
IDBIT result report	As requested by CMTS
ODBIT result report	After the connection is established or as requested by CMTS
Administrative Status	As requested by CMTS
Digital administration response	In response to switching command
Analog administration response	In response to the analog set command
Location Information	As requested by CMTS
Maintenance mode status	As MCCD is taken to maintenance mode
Phasor measurements report	10 Hz
Other measurements report	10 Hz
From MCMS to MCCD	
ODBIT inquiry	After the connection is established to assign ID for the MCCD
Administrative status inquiry	As the switches' status and analog setpoints in the system is queried

Table A2. *Cont.*

Message's Name	Send Frequency
From MCMS to MCCD	
Numerical administration instruction	As the switches' status will be set
Analog administration instruction	As the analog setpoints will be set
Location information inquiry	As requested by CMTS

In Table A2, the phasor measurements report includes:

1. Three-phase voltage magnitude for three channels;
2. Three-phase voltage angle for three channels;
3. Frequency for three channels;
4. Three-phase + neutral, current magnitude for three channels;
5. Three-phase+ neutral, current angle for three channels;
6. Timestamp.

The other measurements report include:

1. Three-phase voltage RMS values for three channels;
2. Three-phase + neuter, current RMS values for three channels;
3. Total apparent power values for each of three channels;
4. Total active power values for each of three channels;
5. Total reactive power values for each of three channels;
6. Three-phase power factor values for three channels.

Appendix A.3. Graphical User Interface Module

Real-time monitoring and manual control are the main purposes for the implementation of the user interface. The UI should provide the opportunity to make the MG operator able to explore the historical data related to the MGCS. Moreover, the operator should be able to observe the corresponding forecasts to renewable generation and load. The Python environment is utilized to implement the proposed UI. For this purpose, several Python libraries are utilized, including "PyQt5", "OpenCV," and "matplotlib." To provide all mentioned capabilities for the user through the UI, a five-tab UI seems necessary. Each of these tabs may include several different sub-tabs. These five tabs are:

1. Main tab;
2. Online monitoring tab;
3. Forecast tab;
4. Data analysis tab;
5. Online control tab.

The main tab includes the following sections:

1. Single-line diagram;
2. MG status;
3. Instantaneous total generation;
4. Instantaneous total load;
5. Power exchange at POI;
6. Instantaneous total renewable generation.

The single line diagram shows the current topology of the medium voltage network and connected DERs. The instantaneous total generation, total load, and total renewable generation sections provide corresponding real power (P), reactive power (Q), and power factor (pf). All values are presented in actual and per unit. MG status shows the current operation mode of the MG and the operating frequency of the MG. In the background, when this tab is opened in the background, the server will send an administrative status check request every 10 s. With the information given by MCCD, the topology of the system will be updated.

In the online monitoring tab, all sub-tab corresponding data are presented in tabulated data format. When this tab is selected, the database's latest data will start to be checked, and the most up-to-date values will be shown on the monitor. The online monitoring tab consists of bus bars, lines, and smart asset (SA) sub-tabs. The pieces of information presented in these sub-tabs are given in Table A3.

Table A3. Description of sub-tabs of GUI's online monitoring tab.

Sub-Tab	Information
Bus bars	Voltage magnitude, voltage magnitude (per unit), voltage phase angle, injection current magnitude, injection current phase angle, real injection power, reactive injection power, apparent injection power, power factor, ON-OFF status if a device is connected to a bus bar
Lines	Current magnitude, current phase angle, real power flow, reactive power flow, apparent power flow, the status of the corresponding CBs
SA	Status of the MCCD, Timestamp of last received data package from MCCD, request ODBIT and IDBIT from MCCDs, last recorded locations of MCCD, SOC of BSS, SOC of connected EVs' batteries

The forecast tab enables the operator to observe the corresponding plotting to renewable generation forecasts and load for the next 24 h. Moreover, the user will be able to export the forecast data. It should be noted that the historical forecast data cannot be reached from this Table. When this tab is opened, the latest forecast results will be copied to local variables, and the graphs will be plotted using these local variables.

The data analysis tab is provided to explore, plot, and export the stored data for the determined time interval. The user determines the acquired time through the corresponding fields. The corresponding sub-tabs are bus bars, forecasts, lines, and smart assets (SA). Bus bars, SA, and Lines sub-tabs provide the historical records of the same data described in the online monitoring table. The forecasts sub-tab enable the user to access the stored forecasted values for the selected unit's generation or load within the determined time interval and comparison with the actual values.

The online control enables the user to perform manual control operations and determine some operations manually or automatically. The user can open and close the switches if he/she wants. When the user selects this operation, the server will send the required Digital administration instructions to the MCCD. Depending on the received information (Digital administration reply), the online diagram will be updated. This enables MGO to execute unplanned islanding. Additionally, the adjustable parameters of the control function, such as the POI power exchange setpoint and time for planned islanding, can be modified.

References

1. Farhangi, H. *Smart Microgrids: Lessons from Campus Microgrid Design and Implementation*; CRC Press: Boca Raton, FL, USA, 2016; ISBN 9781315372679. Available online: https://www.taylorfrancis.com/books/edit/10.1201/9781315372679/smart-microgrids-hassan-farhangi (accessed on 29 October 2021).
2. Marnay, C.; Joos, G.; Iravani, R.; Mancarella, P.; Chatzivasileiadis, S. *Microgrids 1: Engineering, Economics, & Experience*; CIGRÉ: Paris, France, 2015; ISBN 9782858733385.
3. Rocabert, J.; Luna, A.; Blaabjerg, F.; Rodríguez, P. Control of power converters in AC microgrids. *IEEE Trans. Power Electron.* **2012**, *27*, 4734–4749. [CrossRef]
4. Katiraei, F.; Iravani, R.; Hatziargyriou, N.; Dimeas, A. Microgrids management. *IEEE Power Energy Mag.* **2008**, *6*, 54–65. [CrossRef]
5. Karimi, H.; Yazdani, A.; Iravani, R. Negative-sequence current injection for fast islanding detection of a distributed resource unit. *IEEE Trans. Power Electron.* **2008**, *23*, 98–307. [CrossRef]
6. Mukhopadhyay, B.; Das, D. Optimal multi-objective expansion planning of a droop-regulated islanded microgrid. *Energy* **2021**, *218*, 119415. [CrossRef]
7. Olivares, D.E.; Mehrizi-Sani, A.; Etemadi, A.H.; Cañizares, C.A.; Iravani, R.; Kazerani, M.; Hajimiragha, A.H.; Gomis-Bellmunt, O.; Saeedifard, M.; Palma-Behnke, R.; et al. Trends in microgrid control. *IEEE Trans. Smart Grid* **2014**, *5*, 1905–1919. [CrossRef]

8. Palizban, O.; Kauhaniemi, K. Hierarchical control structure in microgrids with distributed generation: Island and grid-connected mode. *Renew. Sustain. Energy Rev.* **2015**, *44*, 797–813. [CrossRef]
9. Ali, N.; Kumar, D. State-of-the-Art Review on Microgrid Control Strategies and Power Management with Distributed Energy Resources. *Lect. Notes Electr. Eng.* **2021**, *693*, 749–756. [CrossRef]
10. Battula, A.R.; Vuddanti, S.; Salkuti, S.R. Review of Energy Management System Approaches in Microgrids. *Energies* **2021**, *14*, 5459. [CrossRef]
11. Rangel, C.M.; Mascarella, D.; Joos, G. Real-time implementation & evaluation of grid-connected microgrid energy management systems. In Proceedings of the 2016 IEEE Electrical Power and Energy Conference (EPEC), Ottawa, ON, Canada, 12–14 October 2014. [CrossRef]
12. Manson, S.; Nayak, B.; Allen, W. Robust Microgrid Control System for Seamless Transition Between Grid-Tied and Island Operating Modes. In Proceedings of the 2015 IEEE Energy Conversion Congress and Exposition (ECCE), Montreal, QC, Canada, 20–24 September 2015; Volume 2015, pp. 1196–1202. [CrossRef]
13. Ameen, A.M.; Pasupuleti, J.; Khatib, T. Simplified performance models of photovoltaic/diesel generator/battery system considering typical control strategies. *Energy Convers. Manag.* **2015**, *99*, 313–325. [CrossRef]
14. Sun, C.; Paquin, J.N.; Jajeh, F.A.; Joos, G.; Bouffard, F. Implementation and CHIL Testing of a Microgrid Control System. In Proceedings of the 2018 IEEE Energy Conversion Congress and Exposition (ECCE), Portland, OR, USA, 23–27 September 2018; Volume 2018, pp. 2073–2080. [CrossRef]
15. Zhao, B.; Zhang, X.; Li, P.; Wang, K.; Xue, M.; Wang, C. Optimal sizing, operating strategy and operational experience of a stand-alone microgrid on Dongfushan Island. *Appl. Energy* **2014**, *113*, 1656–1666. [CrossRef]
16. Carpintero-Rentería, M.; Santos-Martín, D.; Guerrero, J.M. Microgrids Literature Review through a Layers Structure. *Energies* **2019**, *12*, 4381. [CrossRef]
17. The International Electrotechnical Commission (IEC). *Microgrids—Technical Requirements—Protection and Dynamic Control*; IEC 62898-3-1-2020; IEC: Geneva, Switzerland, 2020.
18. The International Electrotechnical Commission (IEC). *Microgrids—Part 2: Guidelines for Operation*; IEC 62898-2-2018; IEC: Geneva, Switzerland, 2018.
19. IEEE Standards Coordinating, IEEE Guide for Design, Operation, and Integration of Distributed Resource Island Systems with Electric Power Systems. 2011. Available online: https://ieeexplore.ieee.org/document/5960751 (accessed on 29 October 2021).
20. IEEE Standard Association. *IEEE Std. 1547-2018. Standard for Interconnection and Interoperability of Distributed Energy Resources with Associated Electric Power Systems Interfaces*; IEEE: New York, NY, USA, 2018.
21. IEEE Power and Energy Society. *IEEE Standard for the Specification of Microgrid Controllers IEEE Standard for the Specification of Microgrid Controllers*; IEEE: New York, NY, USA, 2017. Available online: https://ieeexplore.ieee.org/document/8340204. (accessed on 29 October 2021).
22. IEEE Power and Energy Society. *IEEE Standard for the Testing of Microgrid Controllers*; IEEE: New York, NY, USA, 2018. Available online: https://ieeexplore.ieee.org/document/8319943. (accessed on 29 October 2021).
23. Razeghi, G.; Russ, N.; Samuelsen, S. Generic Microgrid Controller Specifications. In *Technical Report to the US Department of Energy*; National Energy Technology Laboratory: Pittsburgh, PA, USA, 2016; p. 3550.
24. Zadeh, M.R.D.; Mazloomzadeh, A.; Ghaffarzadeh, H.; Castro, H. Model-Driven Microgrid Controller. In Proceedings of the 2019 FISE-IEEE/CIGRE Conference-Living the Energy Transition, FISE/CIGRE 2019, Medellin, Colombia, 3–6 December 2019.
25. Sun, C.; Ali, S.Q.; Joos, G.; Bouffard, F. A Modular Generic Microgrid Controller Adaptive to Different Compositions. In Proceedings of the 2020 IEEE Energy Conversion Congress and Exposition (ECCE), Detroit, MI, USA, 11–15 October 2020; pp. 2472–2479. [CrossRef]
26. Sun, C.; Joos, G.; Ali, S.Q.; Paquin, J.N.; Rangel, C.M.; Jajeh, F.A.; Novickij, I.; Bouffard, F. Design and Real-Time Implementation of a Centralized Microgrid Control System with Rule-Based Dispatch and Seamless Transition Function. *IEEE Trans. Ind. Appl.* **2020**, *56*, 3168–3177. [CrossRef]
27. Ahmed, M.; Meegahapola, L.; Vahidnia, A.; Datta, M. Stability and Control Aspects of Microgrid Architectures-A Comprehensive Review. *IEEE Access* **2020**, *8*, 144730–144766. [CrossRef]
28. Paquette, A.; Harley, R.; Bhavaraju, V.; Krstic, S.; Theisen, P. Design of the fort sill microgrid. In Proceedings of the 2014 IEEE Energy Conversion Congress and Exposition (ECCE), Pittsburgh, PA, USA, 14–18 September 2014; Volume 2014, pp. 4640–4646. [CrossRef]
29. Balaguer, I.J.; Lei, Q.; Yang, S.; Supatti, U.; Peng, F.Z. Control for grid-connected and intentional islanding operations of distributed power generation. *IEEE Trans. Ind. Electron.* **2011**, *58*, 147–157. [CrossRef]
30. Fedele, G.; Picardi, C.; Sgrò, D. A power electrical signal tracking strategy based on the modulating functions method. *IEEE Trans. Ind. Electron.* **2009**, *56*, 4079–4087. [CrossRef]
31. Hunt, C. Overview of TCP/IP-TCP/IP Network Administration, 3rd ed. Available online: https://www.oreilly.com/library/view/tcpip-network-administration/0596002971/ch01.html (accessed on 26 August 2021).